AD-A111 042 BELL AEROSPACE TEXTRON BUFFALO NY F/G 20/5
HYDROGEN PUMPED IODINE LASER STUDY.(U)
JUL 80 J A BLAUER, J W RAYMONDA, D R JANIAK F29601-76-C-0063
UNCLASSIFIED AFWL-TR-79-178 NL

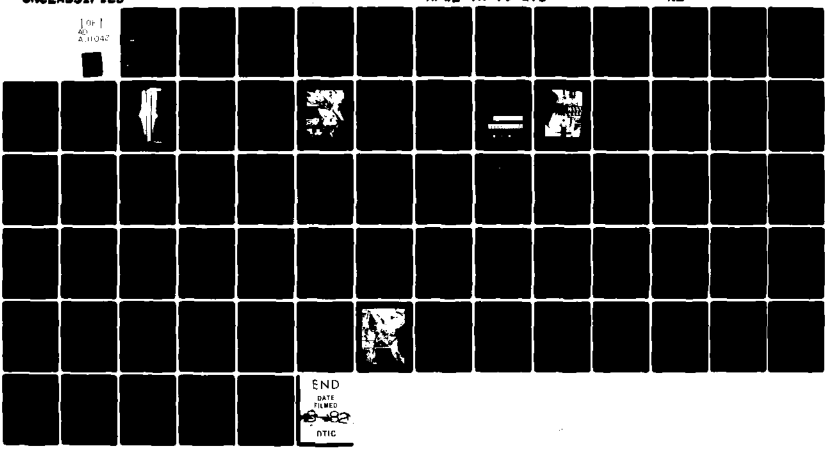

HYDROGEN PUMPED IODINE LASER STUDY

Jay A. Blauer, et al.

Bell Aerospace Textron
Buffalo, NY 14240

July 1980

Final Report

Approved for public release; distribution unlimited.

AIR FORCE WEAPONS LABORATORY
Air Force Systems Command
Kirtland Air Force Base, NM 87117

AFWL-TR-79-178

This final report was prepared by the Bell Aerospace Textron, Buffalo, New York, under Contract F29601-76-C-0063, Job Order 33260310 with the Air Force Weapons Laboratory, Kirtland Air Force Base, New Mexico. Dr. David J. Benard (ARA) was the Laboratory Project Officer-in-Charge.

This technical report has been reviewed and is approved for publication.

David J Benard

DAVID J. BENARD
Project Officer

FOR THE DIRECTOR

Ronald R. Bousek

RONALD R. BOUSEK
Major, USAF
Chief, New Laser Concepts Br

Armand D. Maio

ARMAND D. MAIO
Colonel, USAF
Chief, Advanced Laser Tech Div

UNCLASSIFIED

SECURITY CLASSIFICATION OF THIS PAGE (When Data Entered)

REPORT DOCUMENTATION PAGE		READ INSTRUCTIONS BEFORE COMPLETING FORM
1. REPORT NUMBER AFWL-TR-79-178	2. GOVT ACCESSION NO. AD-A111 042	3. RECIPIENT'S CATALOG NUMBER
4. TITLE (and Subtitle) HYDROGEN PUMPED IODINE LASER STUDY		5. TYPE OF REPORT & PERIOD COVERED Final Report
		6. PERFORMING ORG. REPORT NUMBER
7. AUTHOR(s) Jay A. Blauer, J. W. Raymonda, D. R. Janiak, G. D. Hager, R. Shortridge, G. D. Myers, W. C. Solomon		8. CONTRACT OR GRANT NUMBER(s) F29601-76-C-0063
9. PERFORMING ORGANIZATION NAME AND ADDRESS Bell Aerospace Textron P.O. Box 1 Buffalo, NY 14240		10. PROGRAM ELEMENT, PROJECT, TASK AREA & WORK UNIT NUMBERS 63601F/33260310
11. CONTROLLING OFFICE NAME AND ADDRESS Air Force Weapons Laboratory (ARA) Kirtland Air Force Base, NM 87117		12. REPORT DATE July 1980
		13. NUMBER OF PAGES 70
14. MONITORING AGENCY NAME & ADDRESS (if different from Controlling Office)		15. SECURITY CLASS. (of this report) Unclassified
		15a. DECLASSIFICATION DOWNGRADING SCHEDULE

16. DISTRIBUTION STATEMENT (of this Report)

Approved for public release; distribution unlimited.

17. DISTRIBUTION STATEMENT (of the abstract entered in Block 20, if different from Report)

18. SUPPLEMENTARY NOTES

19. KEY WORDS (Continue on reverse side if necessary and identify by block number)

Atomic Laser
Chemical Pumping
Vibrational Energy
Energy Transfer
Electronic Excitation

20. ABSTRACT (Continue on reverse side if necessary and identify by block number)

Experimental data relative to attempts to induce lasing at 1.3154 μm in a chemical atomic iodine medium are presented.

The critical issue was the establishment of high number densities of hydrogen atoms. First, atomic hydrogen was prepared by shock-heating mixtures of H_2 in Ar. The plenum gases were accelerated through a nozzle bank and molecular HI was injected into the flow. Medium diagnostics were conducted

(over)

DD FORM 1 JAN 73 1473

UNCLASSIFIED

SECURITY CLASSIFICATION OF THIS PAGE (When Data Entered)

20. ABSTRACT (Continued)

in a windowed section downstream of the nozzle exit plane, on both 3 in. and 12 in. nozzle arrays.

All attempts employing the shock tube to induce lasing in this chemical system were unsuccessful and measurements of small signal gain yielded ambiguous results. The major problem was probably loss of hydrogen atoms by wall recombustion.

Following this, a CW approach for the in-situ chemical formation of atomic hydrogen involving reaction between sodium vapor and HI was tested in a flow reactor. Double-resonance gain measurements indicated loss rather than gain. Shock-tube experiments using conditions that previously yielded gain were repeated using the double-resonance gain diagnostic, and only loss was found.

On the basis of these experimental results, it is recommended that efforts to obtain lasing from a hydrogen pumped iodine medium be discontinued.

PREFACE

The work reported in this Technical Report has been monitored by Capt. Russel Armstrong, Maj. William McDermott, and Dr. David Benard of the Air Force Weapons Laboratory (AFWL/ALC). The work was accomplished at the High Energy Laser Research Facilities of Bell Aerospace Textron (BAT) located in Buffalo, New York. Dr. Jay A. Blauer of BAT was the Project Engineer until April, 1979. Dr. John W. Raymonda was Project Manager from April 1, 1979 through the completion of the contract.

The work reported herein covers a time period of forty-one months, beginning in May of 1976 and ending in September 1979.

The facilities and all test equipment described herein were furnished by BAT. The test data described were obtained by Drs. Jay A. Blauer, Gordon D. Hager, Daniel R. Janiak, Warren F. Brandkamp, Robert Shortridge, Gary Myers and John W. Raymonda. The report itself was authored by Drs. Blauer and Raymonda. Special thanks are given to Dr. Leroy Wilson and professor John C. Polanyi who encouraged the beginning of this work, and to Dr. Wayne C. Solomon who aided in the design and interpretation of the initial experiments.

CONTENTS

ILLUSTRATIONS

ILLUSTRATIONS

TABLES

I. INTRODUCTION

1. BACKGROUND

It has been noted by several researchers that, during attempts to produce vibrationally or electronically excited diatomic molecules from highly exothermic reactions of the atom-molecule type, intense atomic resonance line emission is frequently observed.[1-7] Eckstrom et al[1] and Obenauf et al[2] have noted intense emission from electronically excited Mg, Ca, Sr, and Ba during exothermic reactions of the type

$$Ba + N_2O = BaO^* + N_2 \tag{1}$$

Similarly, Cadman et al[3] have observed emission from $I\,(^2P_{1/2})$ during their studies of reactions of the type

$$H + HI = H_2\,(v \leq 3) + I\,(^2P_{3/2}) \tag{2}$$

In the same vein, we have observed emission from $Br\,(^2P_{1/2})$ as derived from a somewhat similar system during the course of our research, i.e.,

$$H + HBr = H_2\,(v \leq 1) + Br\,(^2P_{3/2}) \tag{3}$$

Hall[5] has reported high number densities of electronically excited alkali metal atoms which are formed during reactions of the type

$$Na + F_2 = NaF^* + F \tag{4}$$

Somewhat similar alkali-halogen studies have been reported by Oldenborg et al.[6]

A common feature that appears in the explanation of all of the results referenced is that the atomic emission is of a secondary origin. Thus, M. Polanyi and others[7, 8] postulated multistep excitation mechanisms of the type

$$Na + Cl_2 = NaCl^* + Cl \tag{5}$$

$$Cl + Na_2 = NaCl^* + Na \tag{6}$$

$$NaCl^* + Na = NaCl + Na^* \tag{7}$$

More recently, Polanyi[3] and Husain[9] give the following explanation for the emission at 1.3154 μm observed during the reaction of atomic H and HI, namely that reaction (2) above is followed by

$$H_2(v) + I\,(^2P_{3/2}) = H_2\,(v\text{-}2) + I\,(^2P_{1/2}) \tag{8}$$

1. D.J. Eckstrom, S.A. Edelstein, and S.W. Benson, J. Chem. Phys., 60, 2930 (1974).
2. R.H. Obenauf, C.J. Hsu, and H.B. Palmer, J. Chem. Phys., 58, 4693 (1973).
3. P. Cadman and J.C. Polanyi, J. Phys. Chem., 72, 3715 (1968).
4. M.L. Zwillengerg, D.W. Naegeli, and I. Glassman, Comb. Sci. Tech., 8, 237 (1974).
5. L.H. Hall, Appl. Phys. Lett., 27 (6), 335 (1975).
6. R.C. Oldenborg, J.L. Gole, and R.N. Zare, J. Chem. Phys., 60, 4032 (1974).
7. M. Polanyi, "Atomic Reactions," Williams and Norgate, London, 1932.
8. H. Beutler and M. Polanyi, Z. Physik. Chem., B1, 3 (1928).
9. D. Husain and R.J. Donovan, Adv. Photochem., Vol. 8, pp 1-75, 1971.

Photon yields have been reported for several cases of atomic line emission of the type discussed here and they vary from less than 10^{-6} for some of the cases considered by Eckstron et al[1] to near unity for atomic iodine emission as discussed by Cadman and Polanyi.[3]

Our basic approach to the problem of inducing population inversions among the internal energy states of atomic species by chemical means involves a detailed investigation of candidate secondary processes of the types described here. Our main interest to the present time has been in conducting a detailed study of the chemical and physical processes operative in reactions (2) and (8). We have attempted to induce a population inversion between the $5^2P_{1/2}$ and $5^2P_{3/2}$ states of atomic iodine by chemical means alone. This choice was made, at least in part, due to the fact that much is already known regarding the important chemical kinetic[9,10] and physical processes[11,12,13] of this particular system.

2. MODELING STUDIES

In order to produce useful design information for an experimental approach to a study of the H-HI system, we have collected, from literature sources, the reaction rate data necessary for system modeling attempts. These data are listed in Table I. In constructing this table we use a rate of $1\text{-}5 \times 10^{12}$ cm^3/mol for the V → E transfer process of interest and a theoretical[14] 75% conversion of the exothermic energy of the pumping reaction to vibrational motion in the newly formed H_2 molecule. These values develop from a fit of the kinetic model described here to the data of Polanyi.[3] The collisional deactivation efficiency of H relative to the internal excitation energy of $I(^2P_{1/2})$ is an estimate taken from our recent experiments with these two species. In making these calculations, we have not concerned ourselves with the mixing problem. The results are then of qualitative use only. The line broadening coefficients of Padrick[15] were used in these calculations.

In using the model outlined here we find several interesting features. First, the formation of large quantities of H_2 (v = 3) during the reaction of H and HI does not contribute substantially to the subsequent transfer of vibrational energy to $I(^2P_{3/2})$. This effect has its origins in the near thermoneutral reaction following:

$$H_2(3) + I(^2P_{3/2}) = H + HI$$

Indeed, we find the greatest population of $I(^2P_{1/2})$ under the assumption that most of the H_2 is excited to its second vibrational level. Even with this factor accounted for, we are unable to compute more than a 55% conversion of $I(^2P_{3/2})$ to $I(^2P_{1/2})$ under the conditions investigated, rather then 80% conversion as reported by Cadman and Polanyi[3] (see Figure 1). Nevertheless, it is encouraging to note that although our model underestimates this observed conversion efficiency, it still predicts sizeable small signal gains under obtainable conditions (see Figure 2).

10. D.E. Obrien and J.R. Bowen, J. Appl. Phys., 42(3), 1010 (1971).
11. J.V.V. Kasper and G.C. Pimentel, Appl. Phys. Lett., 5, 531 (1964).
12. K. Hohla and K.L. Kompa, Appl. Phys. Lett., 22(2), 77 (1973).
13. J.V.V. Kasper, J.H. Parker, and G.C. Pimentel, J. Chem. Phys., 43, 1827 (1965).
14. P.J. Kuntz, E.M. Nemeth, J.C. Polanyi, S.D. Roshen, and C.E. Young, J. Chem. Phys., 44, 1168 (1966).
15. T.D. Padrick and R.E. Palmer, J. Chem. Phys., 62, 3350 (1975).

TABLE I. REACTION RATE DATA FOR THE H-HI SYSTEM

REACTIONS INVOLVING GENERALIZED COLLISION PARTNERS

Reaction	M	A	N	E(kcal)	Comments	References
$H + I = HI$	[a] $*/3He + 3H_2$	4.0×10^{17}	-1.0	0.0		16
$I + I = I_2$	$*/250\ I_2$	2.8×10^{14}	0.0	-1.2		17
$H + H = H_2(v)$	$*/2H_2 + 20H$	1.0×10^{18}	-1.0	0.0	$0 < v < 3$	18
$I(^2P_{1/2}) = I(^2P_{3/2})$	10^{-8} He + 10^{-8} Ar 10^{-4} I + 8 HI $6 \times 10^{-4}\ H_2$ + 5×10^{-4} HF [b] 10^{-4} H	7.2×10^{12}	0.5	0.0		9, 19
$H_2(v) = H_2(v-1)$	*	2.5×10^{-4}	4.3	0.0	$0 \leqslant v \leqslant 3$	18
$H_2(v) = H_2(v')$	H	6.9×10^{14}	-0.8	2.2	$v' < v$	20

PUMPING AND EXCHANGE REACTIONS

Reaction	A	N	E(kcal)	Comments	References
$H + HI = H_2(1) + I$	8.0×10^{10}	0.5	0.5		21
$H + HI = H_2(2) + I$	1.4×10^{12}	0.5	0.5		21
$H + HI = H_2(3) + I$	8.0×10^{10}	0.5	0.5		21
$H_2(v) + H_2(v) = H_2(v-1) + H_2(v+1)$	5.4×10^7	1.5	0.0	$0 < v < 3$	22
$H_2(v) + H_2(v+1) = H_2(v-1) + H_2(v+2)$	8.0×10^7	1.5	0.0	$v = 1$	22
$H_2(v) + I(^2P_{3/2}) = H_2(v-2) + I(^2P_{1/2})$	1.5×10^{12}	0.0	0.0	$v \geqslant 2$	c

a This symbol */ signifies that all potential collision partners have unit relative efficiency except those named which have the relative efficiencies given by their coefficients

b This study

c Estimated from data of Reference (3) by comparing the model to it.

16. S W. Benson and T. Fueno, J. Chem. Phys., 13, 1597 (1962).
17. D. Britton, J. Davidson, W. Gehman, and G. Schott, J. Chem. Phys., 25, 804 (1965).
18. R W.F. Gross and J.F. Bott, "Handbook for Chemical Lasers," pp 33-94, Wiley Interscience, New York, 1976.
19. J. A. Blauer, Chemically Pumped Atomic Laser Study, AFWL-TR-75-121, Air Force Weapons Laboratory, Kirtland Air Force Base, New Mexico, March 1975.
20. R.F. Heidner and J.V.V. Kasper, Chem. Phys. Letters, 15, 179 (1972).
21. A.F. Trotman - Dickenson and G.S. Milne, "Tables of Bimolecular Gas Reactions," NSRDS-NB59, U.S. Dept of Commerce, 1967.
22. K.F. Herzfeld and T.A. Litovitz, "Absorption and Dispersion of Ultrasonic Waves," pp 281-282, Academic Press, New York., 1959.

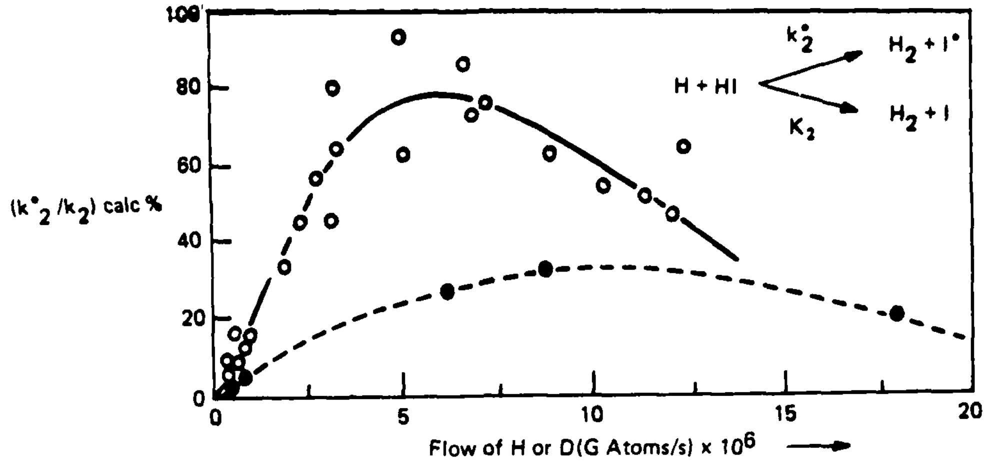

Figure 1. The Apparent Percentage of Reaction Yielding I*. Open Circles Refer to the System H + HI, Closed Circles Refer to D + HI. The Partial Pressure of HI Was ~ 0.34 torr. The Pressure, P_H, Varied to 4 x 10^{-2} torr. (Ref. 3).

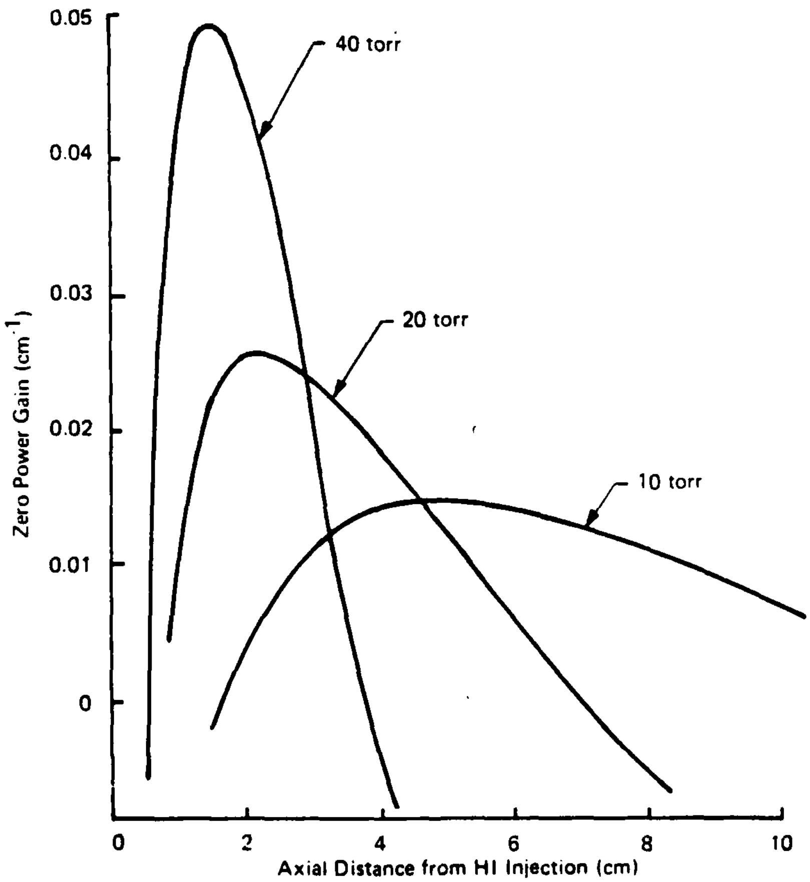

Figure 2. Expected Small Signal Gains at 1.3154 μm Produced in I ($^2P_{1/2}$) By Transfer of Vibrational Energy From Chemically Formed HI

II. EXPERIMENTS

1. PHASE I: THREE-INCH SYSTEM

Since the reaction system of interest requires substantial quantities of atomic hydrogen, we have spent considerable time in developing a source for experimental purposes. Basically, binary mixtures of H_2 and Ar were shock-heated to temperatures in excess of 4500 K, after which the gaseous plenum behind the reflected wave was expanded through a nozzle to a final state in the heighborhood of 300-500 K and 5-15 torr. Gaseous HI was injected into the flow at various positions ranging from the nozzle throat to its exit plane.

Two nozzle types and injection schemes were used in this study. The two approaches are illustrated in Figures 3 and 4. A slot arrangement with HI injection slightly downstream of the throat was used initially. In this arrangement, the nozzle effluent passed directly into the observation region with no attempt to contain the flow. The HI injection was by means of 32 channels, 0.025 cm diameter, top and bottom, leading from a plenum and set at 30° to the nozzle axis. The nozzle had a throat half height of 0.064 cm and an area ratio of 3.8:1. Its total length from throat to exit plane was approximately 1 cm. Materials of construction included stainless steel, aluminum, plexiglass, and nylon. These nozzles also varied from a contoured (bell) slot to a simple wedge, all with the same area ratio. The exit plane width was always 7.5 cm.

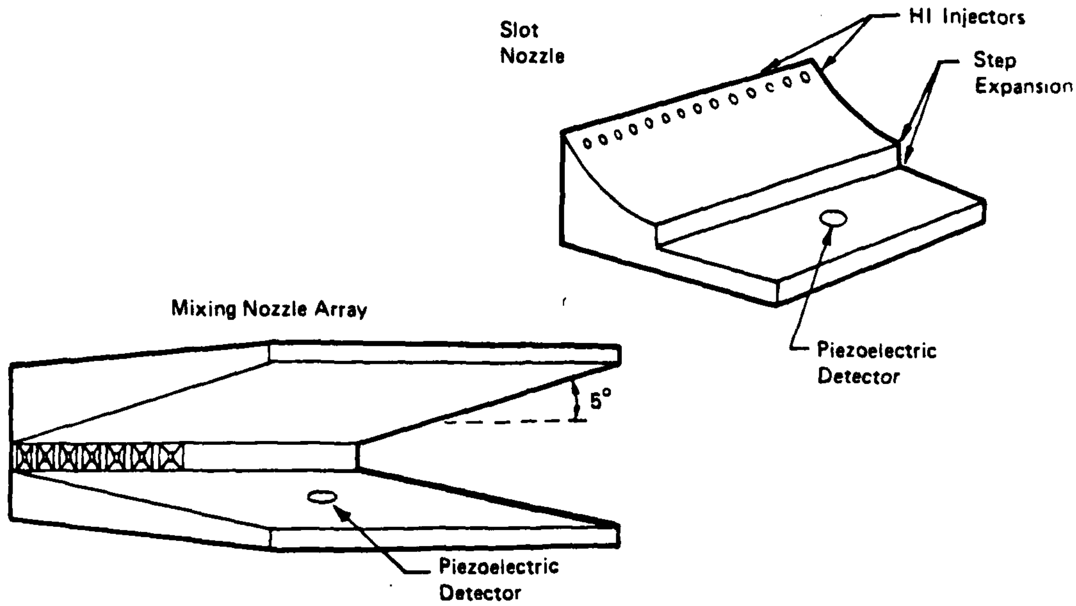

Figure 3. Schematic of Nozzle Designs Used to Study the Iodine Chemical System

The second nozzle design consisted of an array of 23 rectangular nozzles leading from circular throats and interspersed with 24 secondaries for HI injection. The primary nozzles had circular throats of 0.075 cm diameter and an area ratio of 20:1. The secondary nozzles were simple wedges having throat half-heights of 0.013 cm with an area ratio of 5.2:1. The entire array was 7.5 cm wide and was 0.5 cm high. For this particular design, plexiglass shrouds were placed around

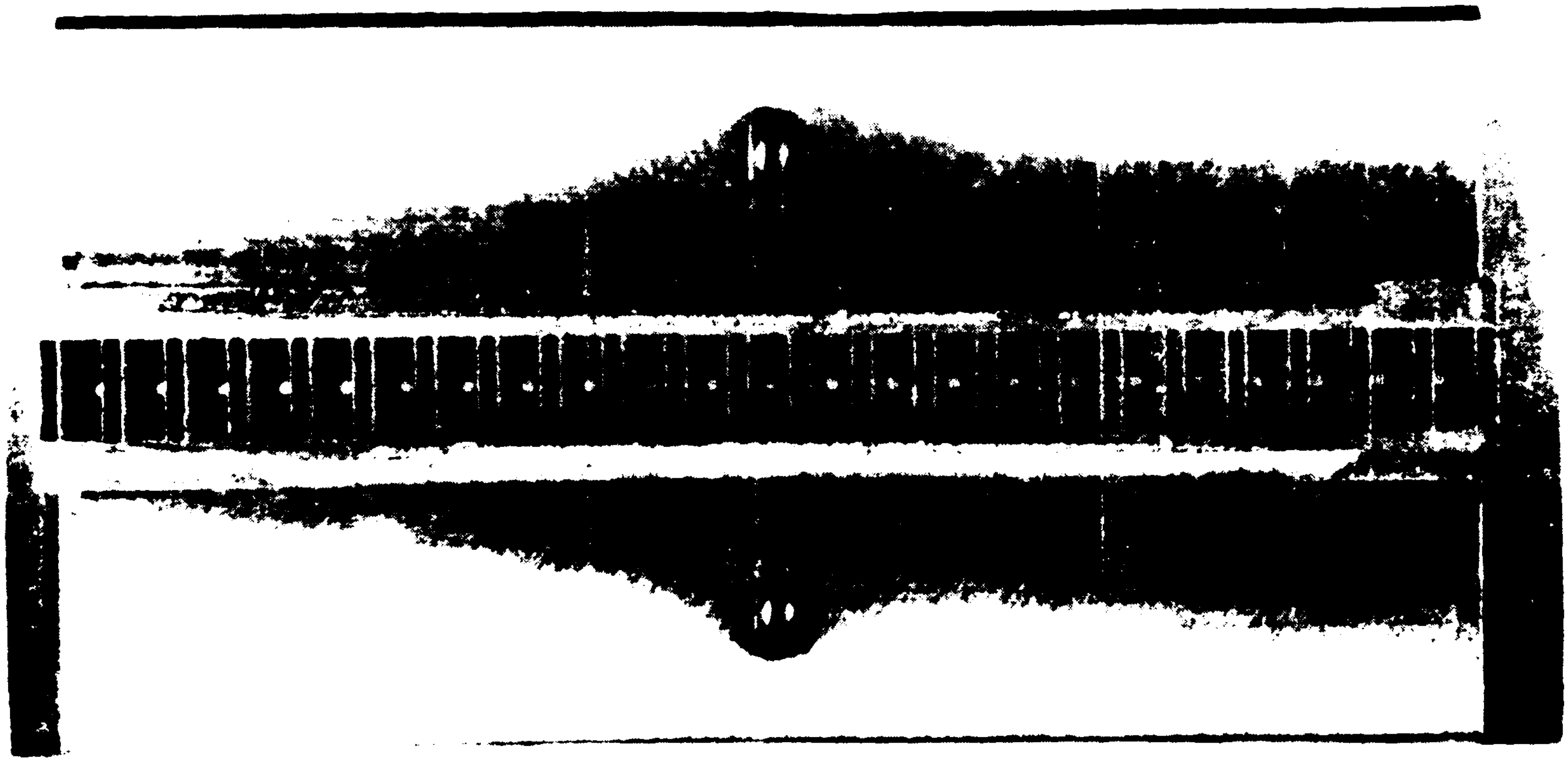

Figure 4. Photograph of Mixing Nozzle Array

the nozzle exit plane to confine the flow. The shroud walls receded from the nozzle at an angle of 5° relative to the flow direction.

The observation section of the apparatus allowed a field of view which extended from the nozzle exit plane to a distance downstream of 5 cm. At this point the flow exited to a vacuum duct having an i.d. of 25 cm and length of several meters and which was continuously evacuated to a pressure less than 0.05 torr.

The shock-tube was of stainless steel and had an inside diameter of 8.9 cm. Shock detection was by means of piezolectric monitors placed along the length of the tube. The driver gas was helium and the driven gas was typically a 3% mixture of H_2 in Ar.

Various diagnostics were used during the course of these studies. Chemiluminescence from $I(^2P_{1/2})$ was observed at several positions downstream of the nozzle exit plane by means of an intrinsic Ge chip detector. Spectral isolation was either by means of a McPhearson 0.333 meter monochromator or a narrow band (±0.04 μm) interference filter centered at 1.3 μm. A comparison of the chemiluminescent intensity with the radiant intensity of a standardized blockbody allowed for a direct estimate of the upper state, $5^2P_{1/2}$, number density. A second diagnostic involved the use of an atomic resonance line absorption technique and gave estimates of both the upper and lower laser level number densities. Thus, optical density measurements at 2062 Å and 1830 Å allowed for number densities of the $5^2P_{1/2}$ and $5^2P_{3/2}$ states to be estimated independently.

The resonance absorption approach required a calibration against carefully prepared standards. These were prepared by dissociation of various compounds of iodine by shock heating of binary mixes in argon. From the equilibrium shock parameters and a pressure measurement (piezolectric) at the observation point within the observation chamber, it was possible to estimate the temperature of the expanded gaseous sample. Thus, from the adiabatic condition,

$$\left(\frac{T_o}{T}\right) = \left(\frac{P_o}{P}\right)^{\frac{\gamma-1}{\gamma}} \tag{9}$$

Here T_o and P_o refer to the plenum conditions; whereas, T and P refer to those existing at the observation point. To make these measurements, the slot nozzle arrangement, Figure 3, was used. The step function within the observation port was eliminated by placement of plexiglass shrouds, the walls of which receded from the flow direction at an angle of 5°. The piezotron (Kistler Mod. 246) was calibrated at the factory for pressure measurements below 1 atm. The calibration was confirmed at our shock tube facility to be accurate to within ±5%.

It is unfortunate that the atomic resonance absorption technique is so very sensitive that it can only be used over a very narrow range of operating conditions. For the $5^2P_{3/2}$ state, concentration measurements can be made with certainty only to the range of 3×10^{-10} mol/cm^3, and for the $5^2P_{1/2}$ state the upper limit is in the range of 3×10^{-9} mol/cm^3. Another source of error which will be most critical for the $5^2P_{1/2}$ state is the assumption that the chemistry and energy transfer processes within the system are frozen on passage through the nozzle.

Finally, late during the program a direct small signal gain measurement was instituted. A probe laser was constructed about a coaxial Xe flashlamp having a bore of 0.25 in., an active length of 5 in., and equipped with coils for water cooling. The windows were of sapphire set at the Brewster angle and the mirrors were AR coated for peak reflectivity at 1.3 μm. The output mirror was flat with a transmissive output coupling of 1% which was used with a total reflector (~99.5%) which had a radius of curvature of 1 m. For an input of 100 J, the device delivered approximately 0.15 mJ with 2 μs FWHM when the lasing fluid was derived from CH_3I at 10 torr pressure. A schematic of the gain measurement is shown in Figure 5, and a photograph of the setup is given in Figure 6. By comparing the ratios of test and reference detector outputs before and during test, it was possible to estimate the gain within the medium during a test. It was found necessary to make the comparison with the ratio of detector outputs obtained for pure shock-heated argon in order to obtain day to day reproducibility.

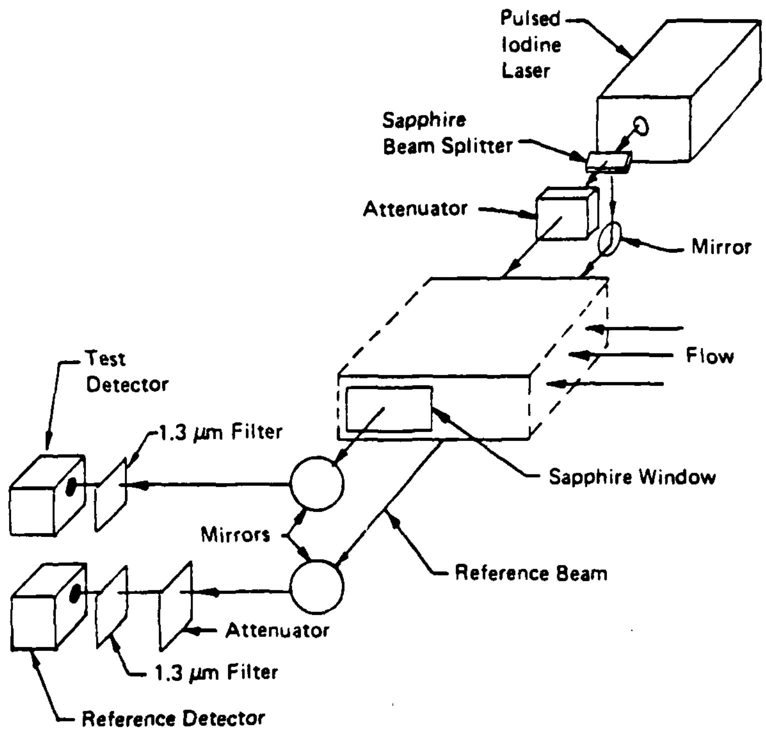

Figure 5. Optical Configuration for Gain Measurements

Initially, a thin (0.0015 in.) Al diaphragm was stretched over the nozzle entrance plane to prevent flow of plenum gases before arrival of the shock wave. The HI flow was initiated 2 s before arrival of the shock wave. Later, it was found that more reproducible results were obtained by initiating a flow of plenum gases through a solenoid valve into the shock tube 2 s before initiation of the shock wave. This latter approach allowed elimination of the Al foil diaphragm which tended to vaporize and condense, mirror like, on the windows. A double diaphragm arrangement allowed for timing of the shock initiation to within 0.5 s.

Gaseous Ar and H_2 were purchased in research grades from Matheson and used without further purification. The HI used was vacuum distilled at 0°C prior to its use. The I_2 and CH_3I were purchased from Malinckrodt at 99.5% purity and used without further purification.

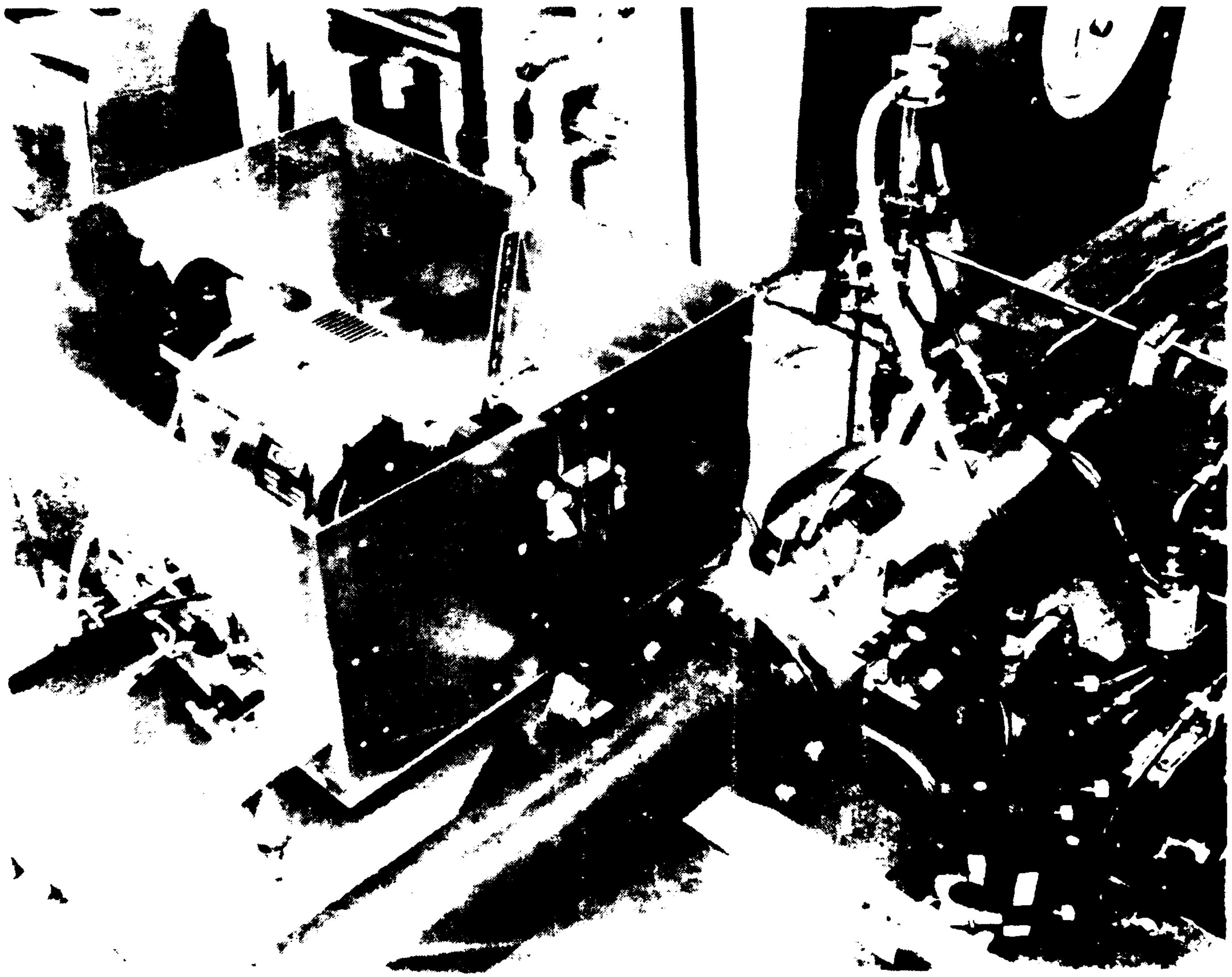

Figure 6. Photograph of Apparatus for Gain Measurement

2. PHASE II: TWELVE-INCH SYSTEM

Gain measurements during Phase I suggested that it would be possible to initiate laser oscillations at 1.3154 μm in a system having a 12-in. gain path. Accordingly, a 12-in. system was designed and constructed. A schematic of the basic equipment is given in Figure 7. A more detailed drawing of the mixing nozzle array that was used is given in Figure 8(a) with a photograph of a small section given in Figure 8(b). A photograph of the assembled apparatus is given in Figure 9.

The nozzle array consists of a double row, the individual elements of which are described here. There are 95 primary nozzles in each row and each is flanked on its two sides by secondary nozzles. The primary nozzles have 0.030-in. diameter circular throats and 0.080 x 0.195-in. rectangular exit dimensions. The overall length of an element (leading from shock-tube plenum) is 0.320-in. The subsonic portion of each element is a 60° conical convergent section of 0.070-in. length. The secondary nozzles are simple wedges having rectangular throats of 0.010 x 0.390-inch cross sections and exit dimensions of 0.035 x 0.390-in. The secondary nozzles are provided with a common feed which was incorporated within the body of the nozzle array and consists of two channels 12-in. long and of rectangular cross section, 0.188 x 0.173-in. The nozzle array is illustrated in Figures 8(a) and 8(b).

The shock-tube is of stainless steel construction and has an inside diameter of 6-3/8-in. The tube is connected to the 12-in.-wide reaction chamber by means of a constant area duct which changes the 6-3/8-inch circular dimension to a rectangular exit of 12 x 2-5/8-inch cross section. The rectangular end of the duct and the reaction chamber are separated by the array of nozzles having an overall rectangular dimension of 0.4 x 12-in. Shock detection is by means of piezoelectric detectors.

The reaction chamber has a rectangular inside cross section with dimensions of 12 x 0.8-in. Aluminum shrouds could be placed within the reaction chamber to provide a smooth transition into the observation area for gases exiting from the nozzle array. In these cases, gases exiting from the nozzle encounter a wall which recedes from the exit plane at an angle of 2°. The observation port extends for 2-in. beyond the nozzle exit plane. The reaction chamber has an overall length of 3-1/2-in. The short length and the subsequent ballast tank (60 gallons) assure proper supersonic operation of the apparatus. Finally, a sensitive piezotron detector is provided for pressure measurements within the reaction chamber at the point of optical measurement. The sensor has a useful range of 0-500 torr with a maximum resolution of 0.5 torr. It has proven necessary to provide high frequency filtering for this device to eliminate, as far as possible, the ringing noise.

The laser cavity was completed as follows: The Brewster windows were of BK-7 glass and had surfaces flat to 1/10 wave at 5461/Å and parallel to 2 s of arc. The surfaces were polished to an LOI tolerance of 00 scratch/dig. The total reflector had a radius of curvature of 2 m and a reflectivity greater than 99% at 1.3 μm. The output coupler was a flat mirror with an Ar coating to give peak reflectivity at 1.3 μm with a transmissivity loss of 1% at this same wavelength. The mirror separation was approximately 85 cm. Detection was by means of a Ge chip intrinsic detector 11 cm beyond the output mirror and coupled to it by means of a metallic tube of 4 in. diameter with nonreflective internal walls. This prevented light leakage around the mirror and into the detector. The most reproducible results were obtained with a freshly cleaned nozzle and injector assembly. Also, it was necessary to use freshly distilled HI. Thus, immediately after steam cleaning the system, a spoiled cavity experiment would be obtained by blocking or detuning the total reflector. The optical arrangement would then be aligned and a tuned cavity experiment would be constructed. The system would then be recleaned.

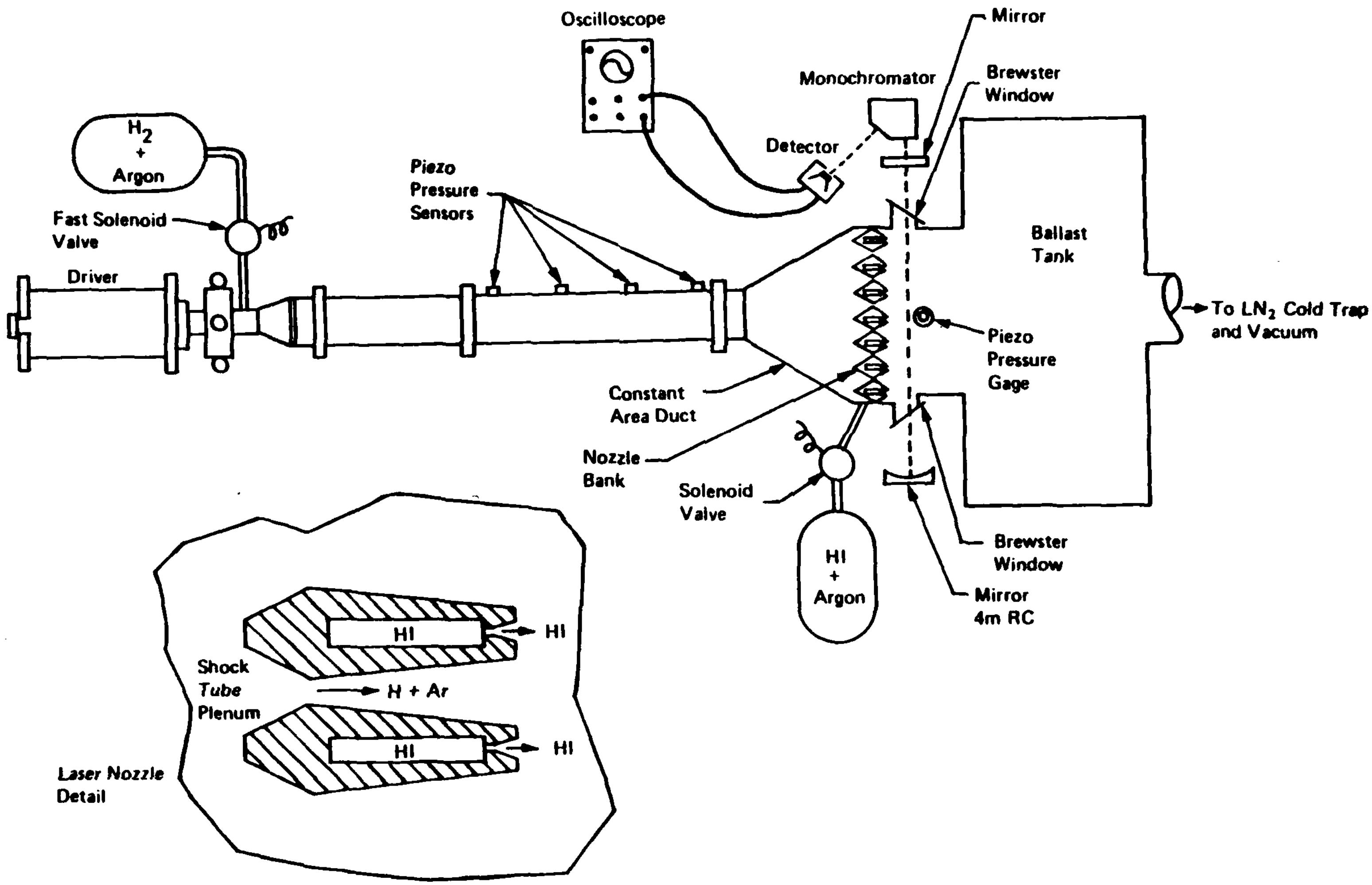

Figure 7. Schematic of Shock-Tube Laser Nozzle Apparatus with 12-Inch Optical Path through Active Medium

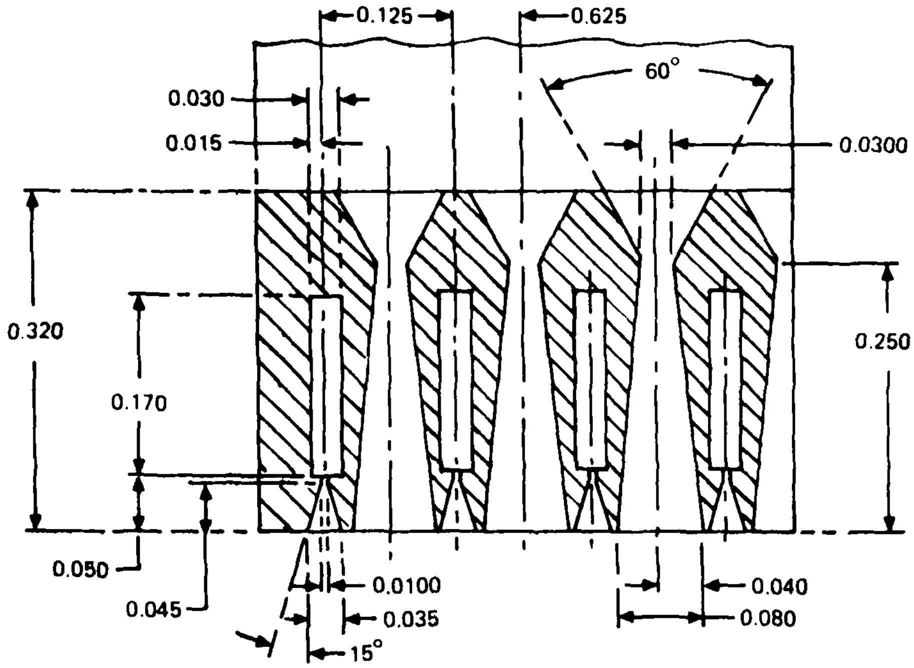

Figure 8(a). Body Nozzle for 12-Inch Shock-Tube Laser

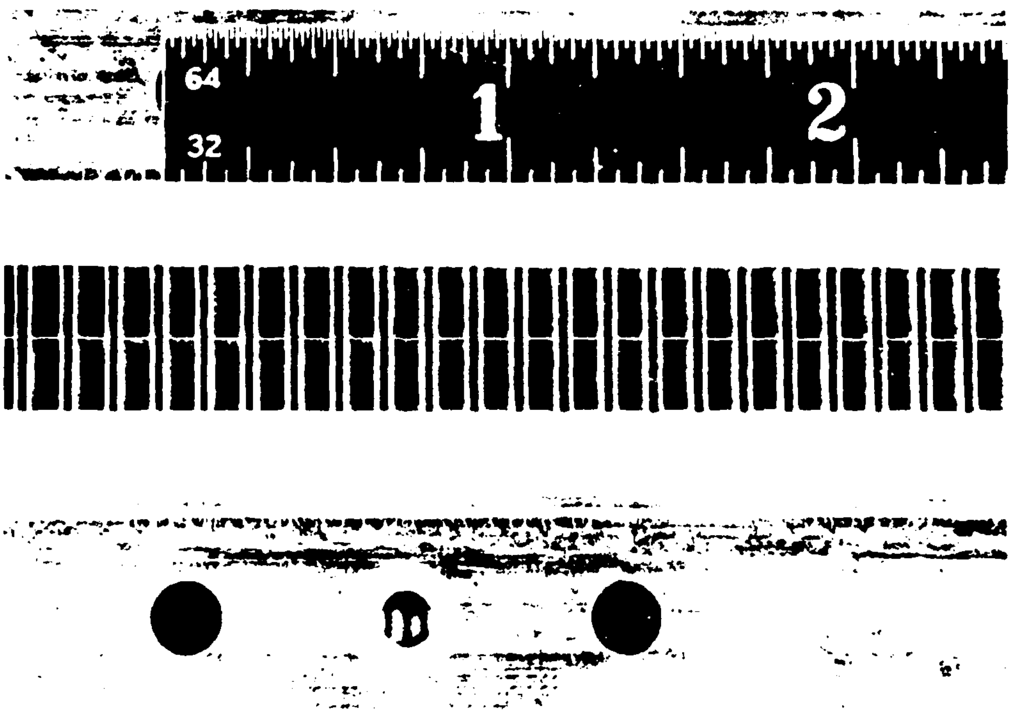

Figure 8(b). Photograph of Mixing Nozzle Array (2½-Inch Section).
Overall Length is 12 Inches

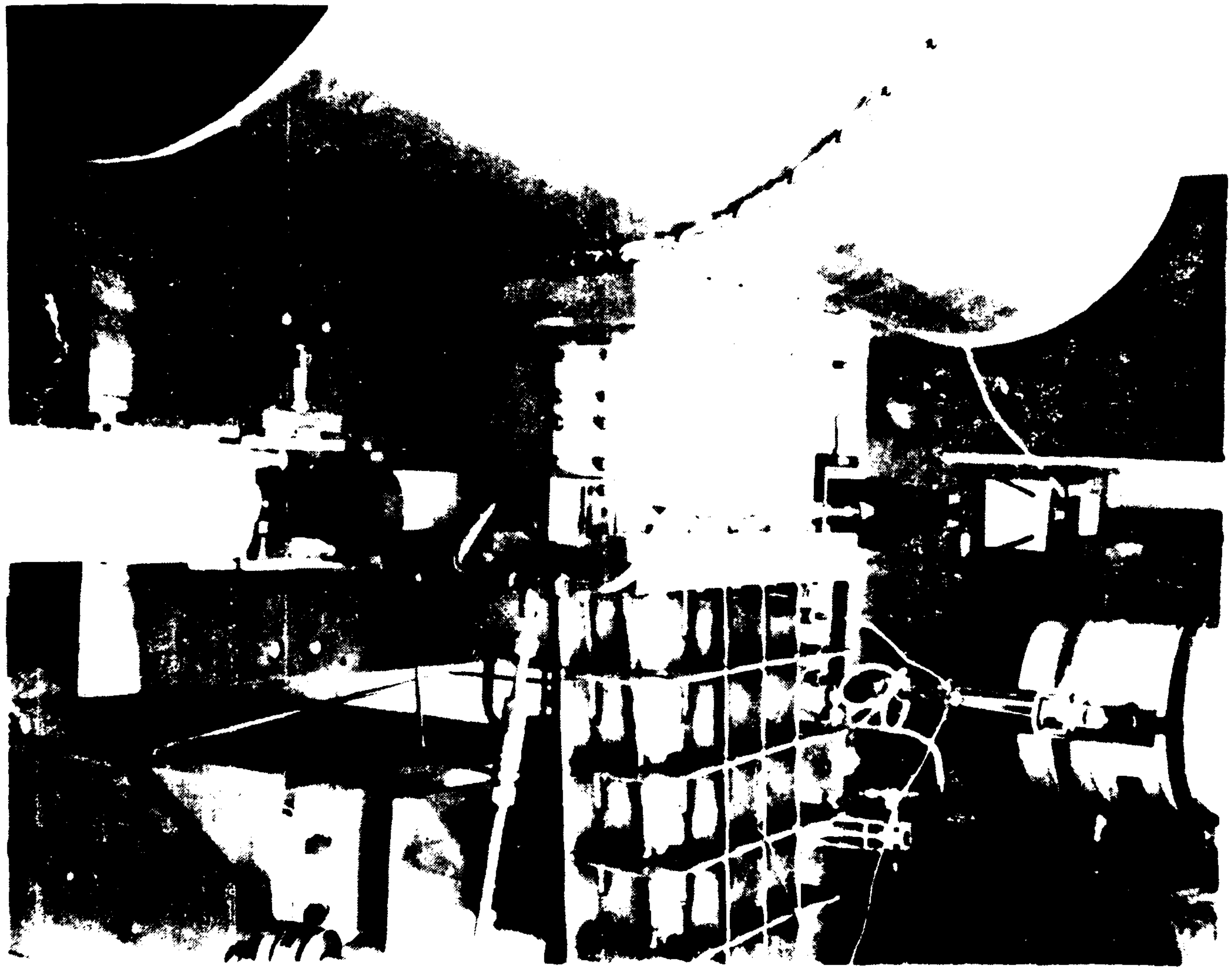

Figure 9. Photograph of Assembled Apparatus Showing the Constant Area Duct, Laser Cavity, and Ballast Tank

3. CALIBRATIONS

For the atomic resonance absorption measurements of iodine atom concentrations, binary mixes of Ar and IF_5, CH_3I, or I_2 were shock-heated to temperatures above their dissociation limit and expanded through the slot nozzle into the test section. A typical optical density and chamber pressure profile is shown in Figure 10 for one case. After an initial transient lasting for about 150 μsec, the chamber pressure approaches its equilibrium value and the measurement can be made, see the figure. The results for these optical density measurements are collected in Tables II and III.

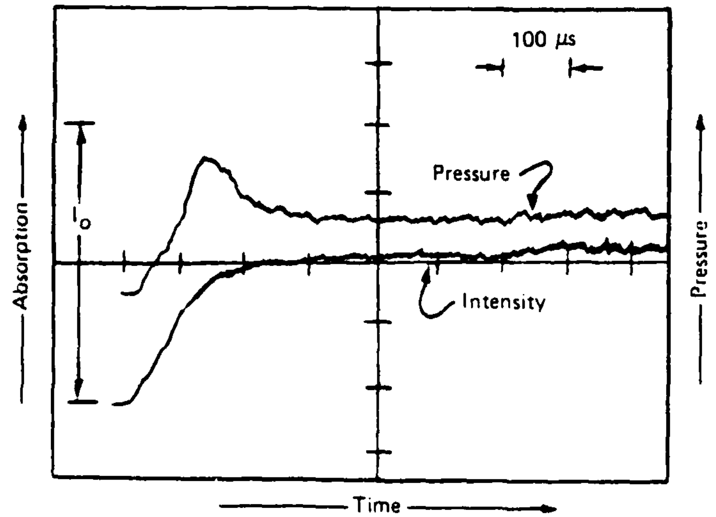

Figure 10. Cavity Absorption and Observation Chamber Pressure Traces for 0.1% IF_5 Shock-Heated to 4160 K and Expanded to 148 torr and 832 K, λ = 1832 Å, Lower State

Since the electronic excitation required for these measurements occurs within the plenum, it is quite possible that due to surface effects within the nozzle, the relative concentration of the $5^2P_{1/2}$ state will be distorted considerably before the point of measurement is reached; on the other hand, due to the relative initial thermal populations, the greatest distortion in the $5^2P_{3/2}$ state that can occur is only about 10%, which is not serious. Accordingly, the calibration presented here can be used with confidence only for the lower ($5^2P_{3/2}$) state and should only be used to indicate the order of magnitude for the upper state ($5^2P_{1/2}$).

A more realistic result for the $5^2P_{1/2}$ state results from the infrared intensity measurements. It can be shown that the concentration of this state is related to the observed intensity level by means of the following equation:[23]

$$N_u = \frac{V/R}{A\,(hc \times 10^{-7}/\lambda)\ \dfrac{a\,wh}{4\pi L}\ g(|\lambda_o - \lambda|)\ \ln\left(\dfrac{L+\Delta L}{L}\right)} \qquad (12)$$

By definition, V is the voltage reading, A the Einstein coefficient[24] (5.4 sec^{-1}), a is the detector cross-section, wh defines the aperture at the window, L is the window (aperture) to detector distance, $g(|\lambda_o - \lambda|)$ is the filter transmissivity at 1.315 μm, ΔL is the optical path length

23. William L. Wolfe, "Handbook of Military Infrared Technology," pp. 457-518, U.S. Govt. Printing Office, 1965

24. V.S. Zuev, V.A. Katulin, V. Yu. Nosach, and O. Yu. Noach, Sov. Phys., JETP, 35, 870 (1972).

TABLE II. ABSORPTION DATA FOR $I(^2P_{3/2})$ AT λ = 1830.4 Å

Precursor	Temperature Plenum	Temperature Expanded	mol/cm^3 $[I(^2P_{3/2})]$	Log (I_o/I)	(cm^3/mol)$^{1/2}$ $\epsilon \ell$
IF_5	5380	1033	1.38×10^{-10}	0.48	4.1×10^4
IF_5	5380	1061	1.47×10^{-10}	0.41	3.4×10^4
IF_5	5000	1065	6.73×10^{-11}	0.41	5.0×10^4
IF_5	5360	1072	3.79×10^{-11}	0.15	2.4×10^4
IF_5	5440	1011	3.35×10^{-11}	0.12	2.1×10^4
IF_5	5500	1033	1.72×10^{-11}	0.11	2.6×10^4
CH_3I	5010	916	3.17×10^{-10}	0.56	3.2×10^4
CH_3I	4880	1021	1.01×10^{-10}	0.30	3.0×10^4
CH_3I	4930	957	4.47×10^{-11}	0.20	2.9×10^4
CH_3I	4960	962	4.44×10^{-11}	0.17	2.5×10^4
CH_3I	4950	993	9.48×10^{-11}	0.28	2.8×10^4
CH_3I	4925	992	5.54×10^{-10}	0.41	1.7×10^4
CH_3I	4925	730	4.71×10^{-10}	0.64	2.9×10^4
CH_3I	4930	730	1.17×10^{-10}	0.21	1.9×10^4
I_2	2445	2445 [a]	6.94×10^{-9}	0.95	$> 1.1 \times 10^4$
IF_5	5440	1067	7.56×10^{-10}	0.56	2.0×10^4

[a] Absorption data taken directly from plenum

TABLE III. ABSORPTION DATA FOR $I(^2P_{3/2})$ AT λ = 1830.4 Å

Precursor	Temperature Plenum	Temperature Expanded	mol/cm^3 $[I(^2P_{3/2})]$	Log (I_o/I)	(cm^3/mol)$^{1/2}$ $\epsilon \ell$
IF_5	3940	720	1.64×10^{-9}	0.26	1.6×10^8
IF_5	3910	703	1.64×10^{-9}	0.34	2.0×10^8
IF_5	3130	699	2.75×10^{-9}	0.59	2.1×10^8
IF_5	3135	810	3.28×10^{-9}	0.61	1.9×10^8
IF_5	4230	927	6.12×10^{-9}	1.13	1.8×10^8
IF_5	3150	715	2.73×10^{-9}	0.49	1.8×10^8
IF_5	4224	1002	7.02×10^{-9}	0.96	1.4×10^8
IF_5	4030	849	3.64×10^{-9}	0.74	2.0×10^8
IF_5	3800	775	3.00×10^{-9}	0.72	2.4×10^8
IF_5	7650	1406	1.59×10^{-11}	0.003	1.9×10^8
IF_5	3820	692	3.87×10^{-9}	0.758	2.0×10^8

The data for the 5 $^2P_{3/2}$ state can be best described by the equation

$$\log\left(\frac{I_o}{I}\right) = (2.9 \pm 0.5) \times 10^4 \left[I\left(^2P_{3/2}\right)\right]^{0.5 \pm 0.07}$$

whereas, for the 5 $^2P_{1/2}$ state, we have

$$\log\left(\frac{I_o}{I}\right) = (1.9 \pm 0.3) \times 10^8 \left[I\left(^2P_{1/2}\right)\right]^{1.0 \pm 0.1}$$

through the medium and wh defines the aperture at the window. The instrument responsivity, R'. is obtained by comparison against a standard black-body source. It can further be shown that [23],

$$R' = \frac{V}{\frac{a\,wh}{L^2} \int_{\Delta\lambda} N_\lambda g(|\lambda - \lambda_o|)\, d\lambda} \tag{13}$$

Where N_λ is the black-body radiancy at wavelength λ and integration is over the spectral bandwidth of the filter.

Gas flow calibrations were accomplished as follows. The gaseous HI, alone or with a diluent, was contained in a 6 liter stainless steel container, within which the pressure was monitored before and after a test. From the flow duration and the pressure drop within the container, the average HI flowrate was easily determined. The flow of plenum gases through the nozzle was assumed to be given by the simple isentropic assumption, i.e., [25]

$$\Gamma = P_o A^* \left(\frac{1}{RT_o M}\right)^{1/2} \sqrt{\gamma \left(\frac{2}{\gamma+1}\right)^{(\gamma+1)/(\gamma-1)}} \tag{14}$$

Here Γ is the molar flow rate, P_o and T_o refer to the plenum, M is the molecular weight, γ is the heat capacity ratio, and A^* is the effective throat area. For our purposes A^* is assumed identical to the geometric area.

25. George Rudinger, "Nonsteady Duct Flow and Wave-Diagram Analysis," pp. 163-168, Dover Publications, Inc., New York, 1969.

III. RESULTS AND DISCUSSION

1. PHASE I: THREE-INCH SYSTEM

Typical absorption traces at both 1830 Å and 2062 Å are illustrated in Figures 11-13. These figures demonstrate conclusively that both reagents (H and HI) are required before I ($^2P_{1/2}$) is formed. Thus, a source derived from simple dissociation of HI in a hot boundary layer can be ruled out. Frequently, infrared emission and uv absorption traces were obtained simultaneously. An example of this is shown in Figure 14. Data taken for the slot nozzle arrangement are collected in Tables IV(a) and IV(b). Where appropriate, the small signal gain was estimated from the measured concentrations by means of the following equation:

$$\alpha = \frac{A\phi_c}{8\pi c\omega_c^2} \left(N_u - \frac{g_u}{g_\ell} N_\ell \right) \tag{15}$$

Here ω_c is the line center frequency (cm^{-1}), N_u and N_ℓ are the number densities of the two states with electronic degeneracies, and ϕ_c is the line function parameter.[26] A Voigt line function was assumed in conjunction with pressure broadening coefficients of Padrick.[15]

A typical infrared trace taken with the mixing nozzle array is shown in Figure 15. Unlike the previous cases, the temporal behavior of the 5 $^2P_{1/2}$ state in this case never exhibits a steady state. Indeed, after a large initial transient, the concentration decays rapidly to near zero. In order to investigate the hypothesis that this is only a reflection of the temporal behavior of the atomic hydrogen delivery, the HI was replaced by F_2 and lasing from HF(v) formed by the following process was sought:

$$H + F_2 = HF(v) + F \tag{16}$$

The windows were of sapphire set at the brewster angle and the mirrors were AR coated for peak reflectivity at 2.7 μm. The output coupling was at 1%. The results are illustrated in Figure 16. The results appear to confirm the hypothesis since the lasing does not attain a steady state value. Nevertheless, the upper state uv trace (not shown) does appear to achieve a steady state condition although this is probably due to a near total absorption. For comparative purposes, it is useful to compare the diagnostic results at a common point in the time history. The point chosen corresponds to the median of infrared intensity. The results are collected in Table V.

Finally, to check the gain estimates obtained by the absorption and emission techniques, a small signal gain measurement was undertaken, Figures 5, 6. In order to reduce the possibility that effects of anomalous dispersion might adversely affect the results, the test detector had an active diameter of 1.9 cm which allowed for complete capture of the entire signal from the probe laser. The results of these measurements are given in Table VI.

---

26. B.H. Armstrong, J. Quant. Spectr., Radiative Transfer, 7(1), 61 (1967).

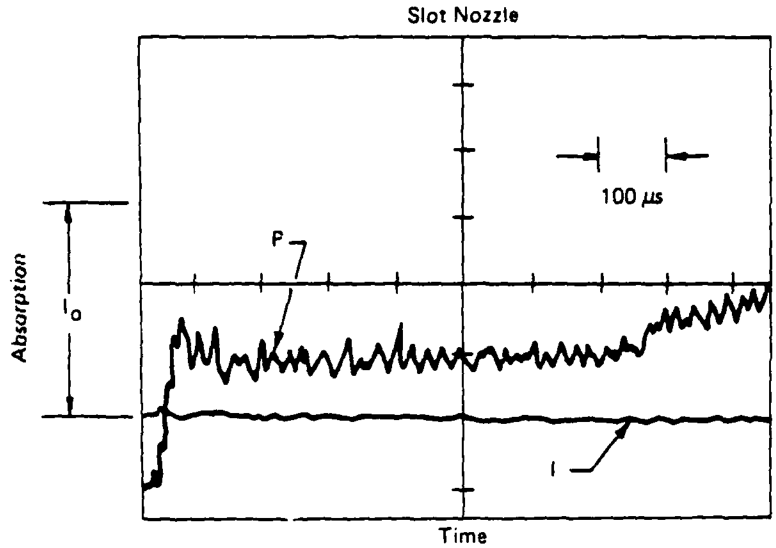

Figure 11. Absorption Profile at 2062 Å for I ($^2P_{1/2}$). Plenum Temperature and Pressure Were 5380 K and 7.2 atm. No HI Was Injected. Initial Mix Was 3% H_2 in Argon. Slot Nozzle

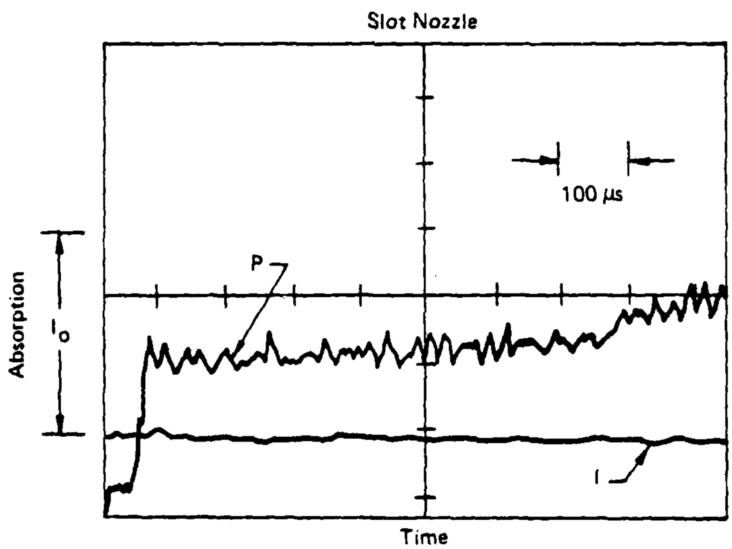

Figure 12. Absorption Profile At 2062Å For I($^2P_{1/2}$). Plenum Pressure and Temp. Were 7.2 Atm and 5380 K Resp. HI Was Injected Downstream. Initial Mix Was 100% Argon Slot Nozzle

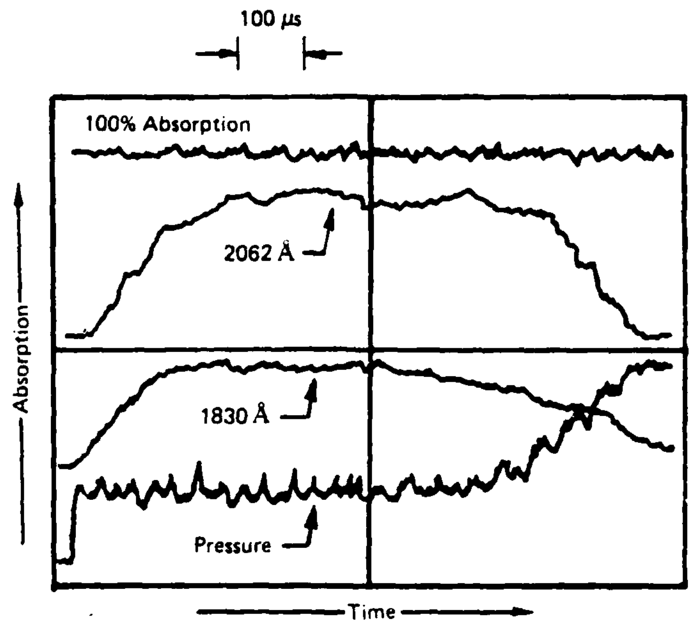

Figure 13. Oscillogram Traces Showing Absorption for the 2062Å and 1830Å Resonance Lines and the Plenum Pressure for One Experimental Condition Having H_2 in the Plenum and HI Injected Downstream. Slot Nozzle

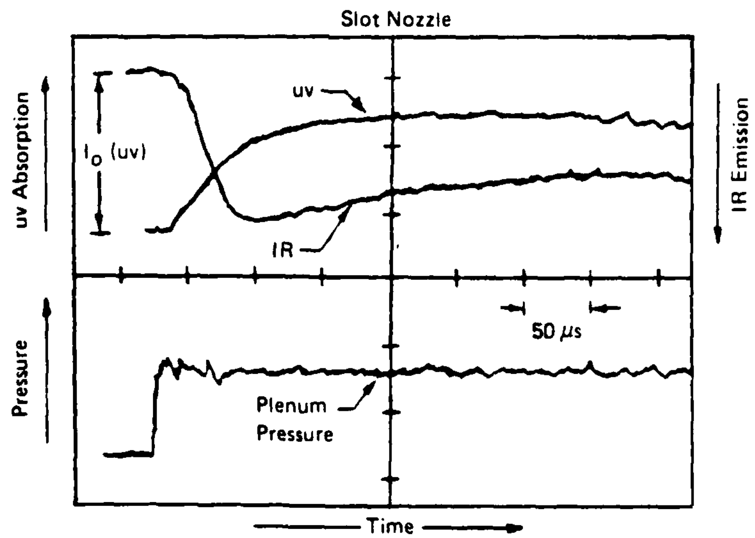

Figure 14. Absorption Profile At 2062Å and Corresponding Emission Trace At 1.3154 μm. Cavity Temperature and Pressure of 475 K and 7.0 torr. Slot Nozzle

TABLE IV(a). EXPERIMENTAL CONDITIONS FOR CAVITY NUMBER DENSITY MEASUREMENTS SLOT NOZZLE

Run	Z^a (cm)	ϕ^b	Plenum Conditions T K	Plenum Conditions P (atm)	P_e^c (atm)	P_c^d (torr)	P_f^e (torr)	X^f (cm)	Y^g (cm)	A^h (cm^2)	log(Io/I) 2062Å	log(Io/I) 1830Å	mol/cm$^{3\,i}$ Nu(uv)	mol/cm$^{3\,i}$ N_L(uv)	mol/cm^3 N_I^j(IR)	α^k (cm^{-1})
1	0.2	0.55	5380	7.6	0.17		9.0	1.0	0.0	3.8	0.637	0.181	3.36×10^{-9}	3.90×10^{-11}		0.012
2	0.2	0.77	5875	5.7	0.12	58	6.8	1.0	0.0	3.8	0.870		4.58×10^{-9}			0.017
3	0.2	0.55	5210	7.4	0.17		8.9	1.0	0.0	3.8	0.768		4.04×10^{-9}			0.015
4	0.2	0.29	6000	8.8	0.19		10.6	1.0	0.0	3.8		0.386		1.77×10^{-10}		
5	0.2	0.25	5150	9.6	0.22	45	11.5	1.0	0.0	3.8		0.505		3.03×10^{-10}		
6	0.2	0.29	5975	8.6	0.19		10.3	1.0	0.0	3.8		0.397		1.87×10^{-10}		
7^l	0.0	2.0	7075	3.0	0.07		3.6	1.0	0.0	3.8					5.2×10^{-9}	0.019
8	0.2	0.80	5850	5.6	0.12		6.7	2.0	0.4	0.16	0.314		1.66×10^{-9}		1.1×10^{-9}	0.006
9^m	0.0	1.1	6050	5.5	0.12		6.6	2.0	0.4	0.16		0.748		6.67×10^{-10}	1.9×10^{-9}	
10	0.2	1.0	7030	7.0	0.16		8.4	2.0	0.0	0.8					1.5×10^{-9}	
11^m	0.0	1.2	6030	5.5	0.12		6.6	2.0	0.0	0.8					1.9×10^{-9}	
12	0.2	4.8	5840	5.6	0.12		6.7	2.0	0.0	0.16	0.16	0.509	8.75×10^{-10}	3.08×10^{-10}	6.3×10^{-10}	0.003
13	0.2	0.39	5370	6.1	0.14	67	7.3	2.0	0.0	0.16	0.258		1.36×10^{-9}			0.005
14	0.2	0.80	5850	5.6	0.12	58	6.7	2.0	0.4	0.16		0.559		3.72×10^{-10}		

a. Axial position of HI injection relative to nozzle throat.
b. Molar ratio of HI flow rate to that of atomic hydrogen.
c. Calculated pressure at nozzle exit plane.
d. Measured pressure in cavity at Z = 3.0 cm.
d. Computed pressure in cavity for fully expanded conditions.
f. Axial position about which measurement is centered within the cavity.
g. Vertical position from center of cavity to center of measurement.
h. Cross sectional area of mask over window.
i. Concentrations of $^2P_{1/2}$ and $^2P_{3/2}$ states of atomic iodine respectively.
j. Concentration of $^2P_{1/2}$ by IR technique.
k. Estimated minimum small signal gain.
l. Plexiglass nozzle.
m. Aluminum nozzle.

TABLE IV(b). EXPERIMENTAL CONDITIONS FOR CAVITY NUMBER DENSITY MEASUREMENTS DATA TAKEN WITH TWO-DIMENSIONAL NOZZLE SYSTEMS

Run	X^a cm	Z^b cm	Plenum Conditions T K	Plenum Conditions P(atm)	Cavity Conditions T K	Cavity Conditions P^c(torr)	ϕ^d	$(HI)^e$ mol/cm³	Log (Io/I) 2062Å	Log (Io/I) 1830Å	Cavity^f Concentrations Nu(uv)	Cavity^f Concentrations NI(uv)	f^g %	mol/cm³ Nu(IR)^h	Nozzle Material	Nozzle Type	α^i cm⁻¹	α^j cm⁻¹
15	1.0	0.0	6700	6.6	856	29	0.6	1.2×10^{8}	0.616		3.2×10^{9}		26		Al	Wedge		
16	1.0	0.0	6690	6.6	856	29	0.7	1.2×10^{8}	0.699	0.356	3.7×10^{9}	1.5×10^{10}	26	4.1×10^{9}	Al	Wedge	0.017	0.015
17	1.0	0.0	6710	6.6	856	29	0.6	1.2×10^{8}	0.700		3.7×10^{9}		30	4.5×10^{9}	Al	Wedge		
18	1.0	0.2	6158	5.4	786	24	1.1	2.1×10^{8}	0.517	0.528	2.7×10^{9}	4.5×10^{10}	15	1.4×10^{8}	Steel	Contour	0.058	0.010
19	1.0	0.2	6570	6.4	834	28	1.0	2.0×10^{8}	0.586	0.383	3.1×10^{9}	1.7×10^{10}	16	1.3×10^{8}	Steel	Contour	0.055	0.013
20	1.0	0.2	6680	6.5	855	29	0.8	1.5×10^{8}	0.398	0.544	2.1×10^{9}	4.8×10^{10}	17	3.3×10^{9}	Nylon	Contour	0.013	0.008
21	1.0	0.2	6650	6.5	849	29	0.7	1.6×10^{8}	0.495	0.490	2.6×10^{9}	2.8×10^{10}	18	2.9×10^{9}	Nylon	Contour	0.012	0.010
22	1.0	0.2	6600	6.4	843	28	0.7	1.6×10^{8}		0.498		2.9×10^{10}			Nylon	Contour		
23	1.0	0.2	6700	6.6	856	29	0.8	1.6×10^{8}	0.511	0.395	2.7×10^{9}	2.5×10^{10}	18	2.7×10^{9}	Steel	Contour	0.011	0.011
24	1.0	0.0	6725	6.6	858	30	0.4	8.3×10^{9}	0.612		3.2×10^{9}		39		Al	Wedge		

a. Distance downstream of nozzle exit plane
b. Injection point relative to throat
c. Computed for optical axis
d. Ratio of molar HI flow to that for atomic H
e. Estimated concentration of HI in cavity before reaction
f. Concentration of $I(^2P_{1/2})$ and $I(^2P_{3/2})$ given by uv absorption measurements
g. Fraction of total I accounted for.
h. Concentration of $I(^2P_{1/2})$ given by IR measurement.
i. Gain calculated from uv measurements
j. Gain calculated from IR measurement

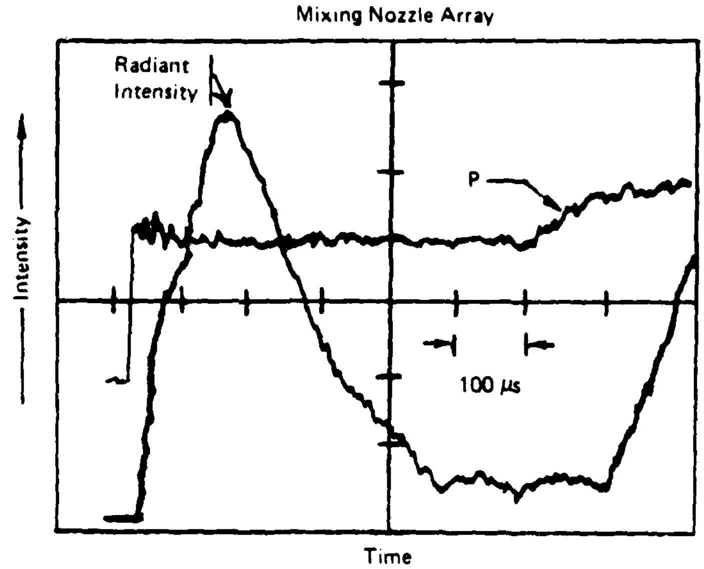

Figure 15. Oscillogram Showing the IR Emission Level at 1.3 μm and the Pressure Profile. Expanded Conditions Were 5.2 torr at 424 K With X_{HI}: X_H: X_{He}: X_{Ar} = 6:5:26:63. Mixing Nozzle Array

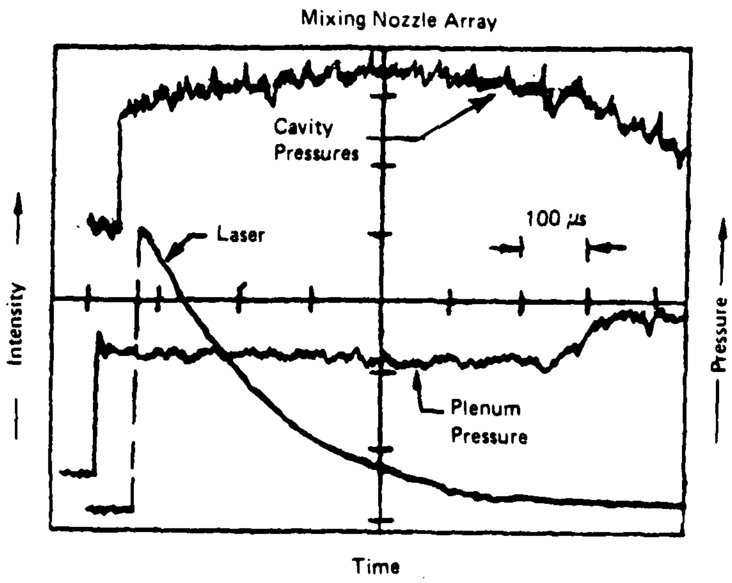

Figure 16. Hot Reaction [$H + F_2 = HF(v) + F$] HF Chemical Laser Action at 2.7 μm. Molecular H_2 Was Dissociated in the Plenum and F_2 Was Injected Downstream. Expanded Conditions of 430 K at 5.2 torr With X_H: X_{F_2}: X_{Ar} = 6:8:89. Mixing Nozzle Array

TABLE V. EXPERIMENTAL CONDITIONS FOR CAVITY NUMBER DENSITY MEASUREMENTS DATA TAKEN WITH MIXING NOZZLE ARRAY

Run	X^a (cm)	ϑ^b	Plenum Conditions T K	Plenum Conditions P(atm)	Cavity Conditions T K	Cavity Conditions P^c	A^d cm^2	$[HI]^e$ mol/cm^3	Log (I_0/I) 2062 Å	Log (I_0/I) 1830 Å	Cavity Concentrations[f] Nu(uv)	Cavity Concentrations[f] Nl(uv)	θ^g %	mol/cm^3 [h] Nu(IR)	Secondary Diluent %	Secondary Diluent Type	α^i cm^{-1}	α^j cm^{-1}
1	1.5	0	5975	8.6	467	7.7	1.7	0	0.0	0.07	0.0	0.0	100	0.0			0.0	0.0
2	1.5	0.71	6000	8.6	469	7.5	1.7	8.2×10^9	0.43		2.2×10^9				14	HE		
3	1.5	0.71	6000	8.6	469	7.5	1.7	8.2×10^9	0.46	0.21	2.4×10^9	7.1×10^{11}	30	1.6×10^9	14	HE	0.016	0.010
4	4.0	0.71	5920	8.6	463	4.0	0.7	5.7×10^9	0.30	0.18	1.6×10^9	5.4×10^{11}	28	8.8×10^{10}	14	HE	0.011	0.006
5	1.5	0.57	5380	10.1	420	8.8	1.7	9.1×10^9	0.53	0.43	2.8×10^9	3.0×10^{10}	34	3.2×10^9	14	HE	0.018	0.026
6	1.5	0.57	5365	10.1	419	9.1	1.7	9.4×10^9	0.40	0.40	2.1×10^9	2.6×10^{10}	25		14	HE	0.013	
7	1.5	0.50	4770	10.8	373	9.7	1.7	1.0×10^8	0.27		1.4×10^9		14		14	HE		
8	1.5	0.55	4950	10.1	387	9.0	1.7	9.7×10^9	0.35		1.8×10^9		19		14	HE		
9	1.5	0.49	5320	9.9	416	8.7	1.7	8.0×10^9	0.40		2.1×10^9		26	2.4×10^9	14	HE		
10	1.5	0.80	5180	9.6	405	8.4	1.7	1.3×10^8	0.38		2.1×10^9		15		28	HE		
11	1.5	1.0	5160	9.5	403	8.3	1.7	1.4×10^8	0.38		2.1×10^9		16		14	HE		
12	1.5	0.36	5250	8.5	410	8.5	1.7	5.3×10^9	0.24		1.3×10^9		24		7	HE		
13	2.4	0.57	5250	9.8	410	8.6	2.0	9.1×10^9	0.45	0.26	2.4×10^9	1.1×10^{10}	27	1.0×10^9	14	HE	0.016	0.006
14	1.5	∞	5820	8.7	455	7.8	1.7	8.5×10^9	0.14		7.4×10^{10}		9		14	HE		
15	1.5	∞	5360	10.9	419	9.8	1.7	9.4×10^9	0.11		6.0×10^{10}		6		14	HE		
16	1.5	0.31	5200	9.7	406	8.5	1.7	5.0×10^9	0.62	0.48	3.2×10^9	3.7×10^{10}	73	8.8×10^{10}	14	CF_3Cl	0.020	0.005
17	1.5	0.29	5300	9.9	414	9.9	1.7	5.1×10^9	0.63	0.51	3.3×10^9	4.2×10^{10}	74	7.1×10^{10}	14	CF_3Cl	0.021	0.003
18	1.5	0.56	5330	9.9	410	6.0	1.0	6.2×10^9						4.4×10^{10}	14	N_2		

a. Distance downstream of nozzle exit plane
b. Molar ratio of HI flow to that for Atomic H
c. At optical axis
d. Cross-Sectional area of optical aperture
e. Estimated concentration of HI in cavity before reaction
f. Molar concentrations of $I(^2P_{1/2})$ and $I(^2P_{3/2})$ resp.
g. Percent of total iodine accounted for by uv measurements.
h. Median concentration of $I(^2P_{1/2})$ from IR intensity.
i. Gain calculated from uv measurements.
j. Gain calculated with IR measurements.

TABLE VI. SMALL SIGNAL GAIN MEASUREMENTS TAKEN WITH THE MIXING NOZZLE ARRAY (TRIPLE PASS)

Plenum Conditions		Cavity Conditions				Corrected[b]	
T K	P(atm)	T K	P(torr)	ϕ[a]	$\alpha\ell$	$\alpha\ell$	α
5380	10.1	359	8.8	0.0	-0.12	0.0	0.0
4110	9.2	250	6.4	c	-0.31	-0.27	-0.035
5250	8.5	370	8.5	0.7	+0.06	+0.18	+0.008
5350	9.4	334	6.9	0.7	+0.02[d]	+0.06	+0.008
5030	9.0	337	8.8	0.7	+0.02	+0.14	+0.006
5200	9.0	325	6.7	0.7	+0.09	+0.21	+0.009
5350	9.4	334	6.9	0.7	+0.0	+0.12	+0.005

[a] $\phi = \dot{n}_{HI}/\dot{n}_H$

[b] corrected for Ar blank

[c] 5% CH_3I in Ar with single pass

[d] single pass

Also listed in Table VI are the results obtained when a 5% mix of CH_3I in Ar is shock-heated to 4110 K and accelerated through the nozzle. The result is for a single pass and is indicative of the fact that the probe laser is oscillating at a frequency that can interact with atomic iodine within the cavity. Furthermore, a computation of the expected loss within this medium, equation (15), indicates a value of approximately -0.05 cm^{-1} in fair agreement with the -0.035 observed.

The first result given in Table VI is indicative of the losses within the medium itself. Thus, in the absence of HI, the shock treated gases exhibited a loss of 4% per pass. It was found later that this effect could be reduced by approximately half by dispensing with the aluminum foil diaphragm in front of the nozzle as described in the experimental section. When the data in the table are corrected for this effect, apparent gains in the neighborhood of 0.01 cm^{-1} are obtained. These results are then not inconsistent with the results found in Tables IV and V.

Finally, before a thorough lasing demonstration is undertaken, these results suggest that much effort must be spent in overcoming the observed medium losses. Also, the low gain nature of this iodine chemical system ($\alpha \ell \sim 0.02$) suggests that a longer path through the medium is needed. To accomplish this, the path length was increased from 7.5 cm (Phase I) to 30 cm (Phase II), see below.

In order to demonstrate more conclusively that the nonsteady behavior in the performance of the nozzle array is a specific function of the chemistry and physics of the hydrogen atom, the following experiment was performed. A binary mixture of SF_6 and Ar was shock-heated to a temperature of 5825 K and expanded through the nozzle array. Gaseous H_2 was injected into the flow through the secondary nozzles and lasing from HF(v) formed by the following process was sought:

$$F + H_2 = HF(v) + H \tag{17}$$

The result is illustrated in Figure 17. The laser signal very quickly achieves a steady state which is maintained to the end of the test. This indicates that the loss in signal mentioned above is due to a loss in the H atom number density and is probably not grossly affected by gas dynamic considerations.

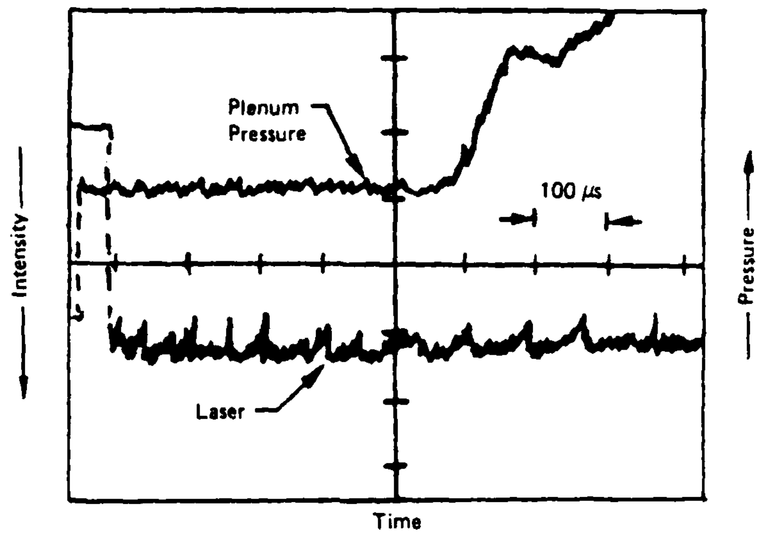

Figure 17. Cold Reaction [F + H_2 = HF(v) + H] HF Chemical Laser Action at 2.7 µm. Molecular SF_6 Was Dissociated In the Plenum and H_2 Was Injected Downstream. Expanded Conditions of 377 K and 9 torr with X_F: X_{H_2}: X_{Ar} = 3:5:92

A comparison of the results for these two nozzle systems indicates that although the nozzle array does not generate steady state conditions, it does give a higher peak density for the $5^2P_{1/2}$ state. This suggests that a lasing demonstration will probably be more successful with this system. A likely partial explanation of these comparative results is that the nozzle array provides better mixing of the reagents on the one hand, and on the other hand, provides a greater surface area in both the subsonic and supersonic regions for H atom recombination. An alternative explanation of the initial transient is based upon the fact that initially the nozzle elements and cavity are flooded with HI. This is rapidly swept out of the way and an efficient turbulent mixing of reagents is replaced by a laminar mixing which is less efficient.

2. PHASE II: TWELVE-INCH SYSTEM

Typical pressure histories within the plenum as well as at the center of the observation (windowed) section are shown in Figure 18. The plenum transducer is located 4.25 in. off center and 2 in upstream of the nozzle bank. It is to be noted that the cavity transducer shows a positive response about 50 µs before the upstream plenum transducer registers the reflected wave. (This is due to the fact that the transducer is 5.5 cm upstream of the end wall with the scope being triggered by passage of the reflected wave.)

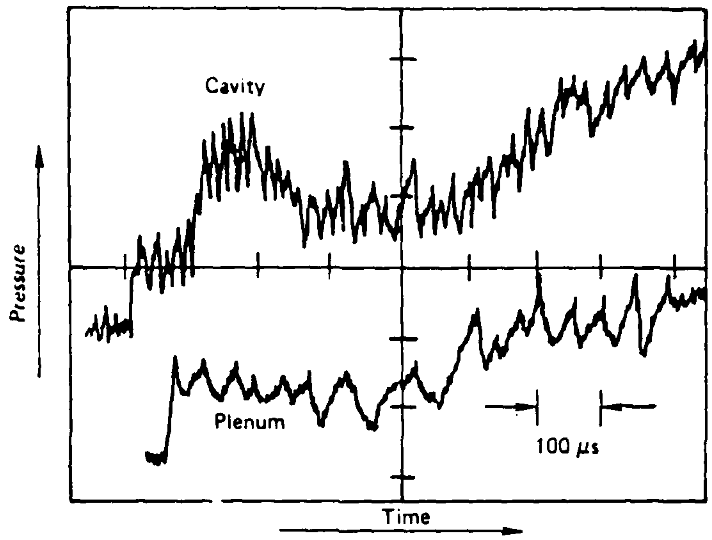

Figure 18. Illustration of Cavity and Plenum Pressures as a Function of Time for the 12-Inch System. Reflected Shock Parameters of 3960 K and 2.9 Atm

A typical chemiluminescent trace for conditions reasonably close to those cited in Figure 18 is shown in Figure 19. The result is very similar structurally to that obtained with the smaller, 3 in. device described previously, see Figure 15. The maximum chemiluminescent intensity occurs in the vicinity of the maximum cavity pressure, see Figure 18. The total width of the chemiluminescent pulse is only 250 μs which suggests that uncertainties in shock-structure within the plenum will heavily influence the results shown here. An interesting feature of these results is that they are reproducible only in a newly steam cleaned nozzle and injector assembly and with freshly distilled HI.

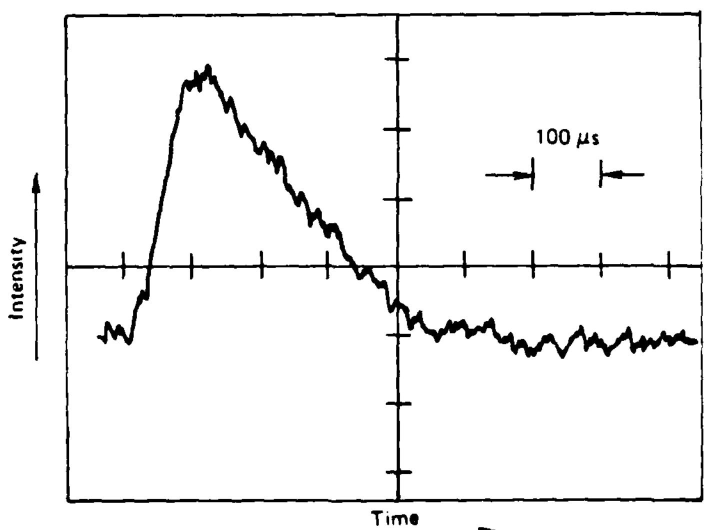

Figure 19. Illustration of Typical Chemiluminescent Pulse Produced in 12-Inch System. Plenum Conditions Were 3820 K and 3.1 Atm. Initial Cavity Conditions Correspond to X_{Ar}: X_{HI}: X_H = 79:16:5 at 22 torr

Thus, after the first test, the luminescent intensity degrades rapidly, see Figure 20. This is not surprising in view of the fact that after each use the injector assembly is contaminated with solid iodine resulting from decomposition of HI on the freshly cleaned steel surfaces.

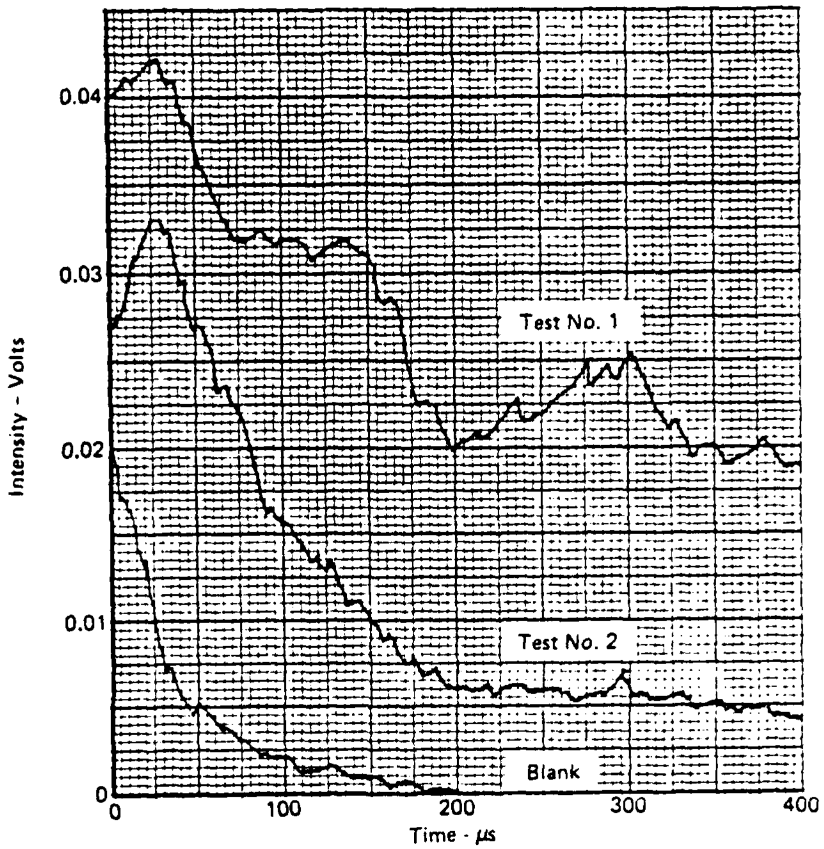

Figure 20. Illustration of Effects of Injector Contamination on Chemiluminescent Intensity. The Duplicate Tests Were for a Plenum of 5.8% Atomic H in Ar at 3900 K and 3.5 atm With HI Injection

Several attempts to induce laser oscillations within the chemically produced medium were made during the course of these studies. Typical results are shown in Figures 21 and 22. The spoiled cavity results were obtained by simply detuning the total reflector. While these results certainly indicate a resonant interaction within the cavity, they are not indicative of laser action. Indeed, a few experimental conditions gave results indicating even less mirror enhancement than shown here, see Figure 23. That laser action can be induced in a satisfactory medium within the apparatus as described is demonstrated by the results illustrated in Figure 24. Here oscillations at 2.7 μm are induced in an HF medium produced by the hot reaction chemistry, see also Figure 14 for comparative purposes. Although laser oscillations can be induced in HF when tested in the 12-in. device described here, power measurements gave disappointing results (less than 10 W).* When modeled, this experimental condition indicates the potential for several hundred watts. Evidently, the lasing medium has been prepared in a far from optimal manner. This is likely a further reflection of the causes that give a nonsteady H-atom flux, see Figure 23.

* Scientech model 342 pulsed power meter used.

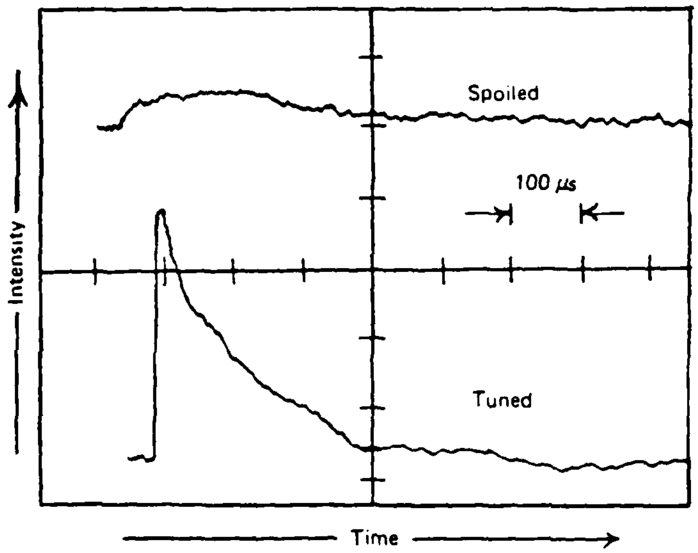

Figure 21. Illustration of Cavity Experiments for One Experimental Condition. Plenum Conditions Correspond to 3825 K and 3.2 Atm. The Measured Cavity Pressure Was 30 torr With X_{Ar}: X_{HI}: X_H = 86:11:3

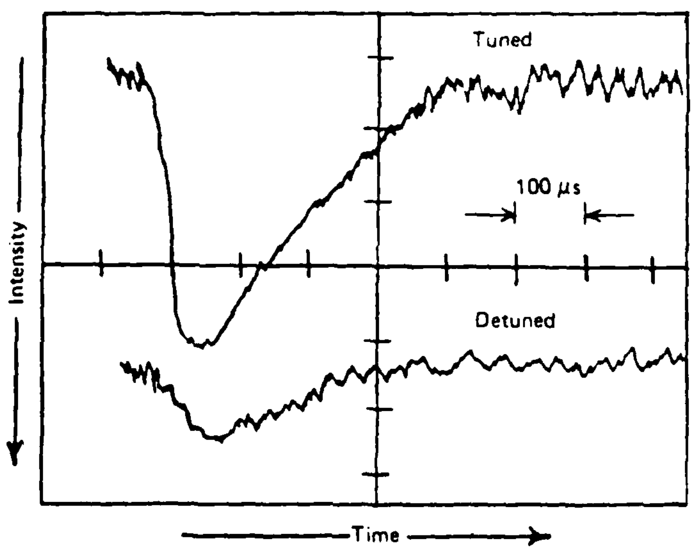

Figure 22. Illustration of Cavity Experiments for One Experimental Condition. Plenum Conditions Correspond to 3820 K and 3.1 Atm. The cavity Pressure Was 30 torr With X_{Ar}: X_{HI}: X_H = 84:11:5

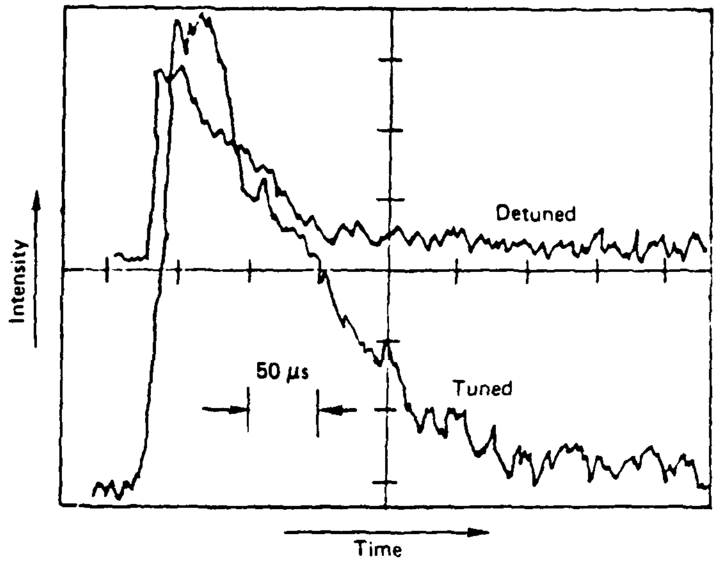

Figure 23. Illustration of Cavity Experiments for One Experimental Condition. Plenum Conditions Correspond to 3730 K and 3.2 Atm. The Measured Cavity Pressure Was 22 torr With X_{Ar}: X_{HI}: X_H = 75:20:5

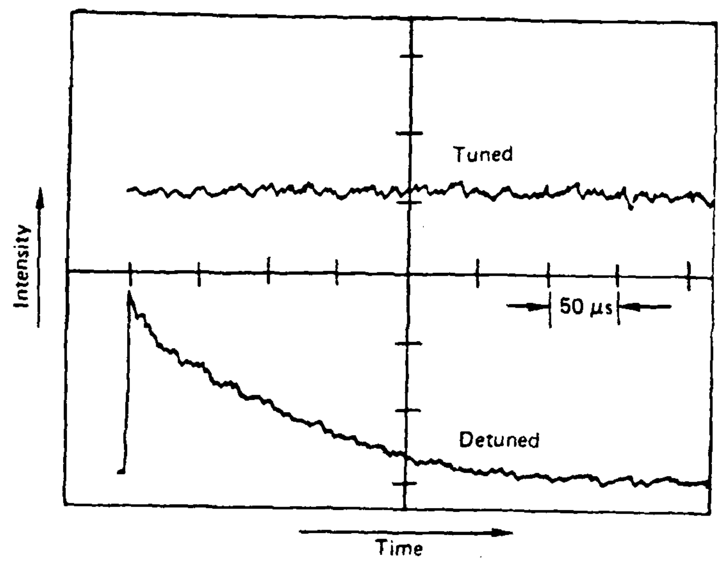

Figure 24. Illustration of Hot Reaction [$H + F_2 = HF(v) + F$] HF Chemical Laser Action At 2.7 μm. Molecular F_2 Was Injected Downstream. Cavity Conditions Correspond to 9 torr With X_{Ar}: X_{F_2}: X_H = 93:1.5:5.5

Since the attempts to induce laser oscillations within the chemically prepared medium were unsuccessful, it was decided to regress one step to conduct a series of gain measurements. During the course of these experiments, it was found necessary to place the germanium detectors at least a distance of 16 ft from the windowed section to prevent any interference with the measurement due to spontaneous emission. Furthermore, in line with the results obtained for the luminescent studies, the measured gain decreased in a regular fashion with each succeeding test after the apparatus was cleaned and the HI was redistilled, see Table VII. The oscilloscope traces obtained for a typical gain measurement are illustrated in Figures 25(a) and 25(b). The results given in Figure 25(a) reflect the conditions existing in the quiescent unshocked gas and were used as the reference point for the actual gain measurement which is shown in Figure 25(b). Typically, the uncertainty in these measurements was found to have an absolute value of approximately ±0.03 as evidenced from the ratios obtained by several individuals independently for a single experiment. The results, while marginal, do indicate that in a few instances positive gain may have been observed.

TABLE VII. SMALL SIGNAL GAIN MEASUREMENTS FOR 12 INCH-SYSTEM SHOWING EFFECT OF INJECTOR AND NOZZLE WALL CONTAMINATION

	Plenum Conditions		Cavity Conditions				
Test [a]	T K	P (atm)	T °K	P (torr)	ϕ^b	$\dot{n}_{HI}$ (mol/s)	α_{ℓ}^{c}
1	3450	2.9	610	22	4.3	0.143	-0.18
2	3600	3.0	562	22	4.0	0.129	-0.40
3	4100	3.7	667	30	3.1	0.136	-0.37
Blank	3490	2.8	560	22	0.0	0.000	+0.01
1	3440	2.9	480	16	0.6	0.024	-0.03
2	4240	3.6	697	30	2.3	0.129	-0.37
3	3580	2.7	583	22	4.3	0.129	-0.55
1	3600	1.2	667	9	1.6	0.021	+0.10
2	4000	1.8	536	9	1.0	0.019	-0.20
1	4040	1.7	559	9	1.1	0.021	+0.10
1	4110	1.6	569	9	1.3	0.021	+0.04
2	4200	1.5	606	9	1.2	0.021	-0.12

[a] Number of tests since system was cleaned and HI was redistilled.
[b] Molar ratio of HI flow to H-atom flow, equation (14).
[c] Single pass gain

Several nozzle blockage experiments were conducted during the course of these investigations. Metallic tape strips were placed over selected blocks of the primary nozzle inlets. An overall comparison of the results should allow for the development of much useful information regarding the dynamic behavior of the medium within the cavity flow region. In the first instance, tape strips were placed over the first 4 inches on each side of the center, only the central one third of the nozzle bank being left clear. A simple chemiluminescent experiment was then conducted and compared with the corresponding result for an unblocked system, see Figure 26. The nearly identical traces are indicative of a very nonuniform condition existing within the medium probably due, at least in part, to wall effects within the plenum. It should be possible to reduce these effects by raising the plenum temperature and pressure.

Several other nozzle blocking experiments were conducted with the cold reaction of the H_2-F_2 chemical laser as the principal diagnostic. Mixes of SF_6 and argon were dissociated in the plenum and H_2 was injected into the flow within the laser cavity. Typical results are illustrated in Figures 27 and 28 and tabulated in Table VIII. At least two interesting features are immediately

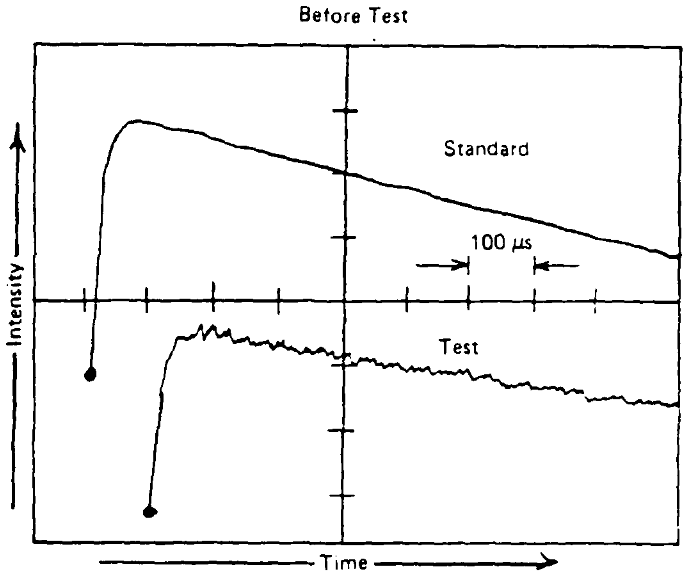

Figure 25(a). Illustration of Pregain Reference Measurement In 12-Inch System for One Experimental Condition, See Fig. 23(b). Before Test

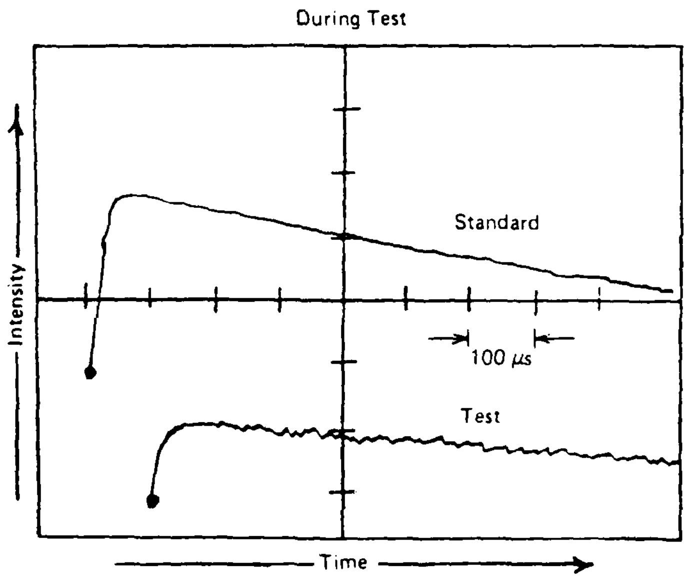

Figure 25(b). Illustration of Gain Measurement In 12-Inch System. Plenum Conditions Were 4100 K and 3.7 Atm. Cavity Pressure Measured at 22 torr With X_{Ar}: X_{HI}: X_H 80:14:6. A 35% Loss Is Recorded. During Test

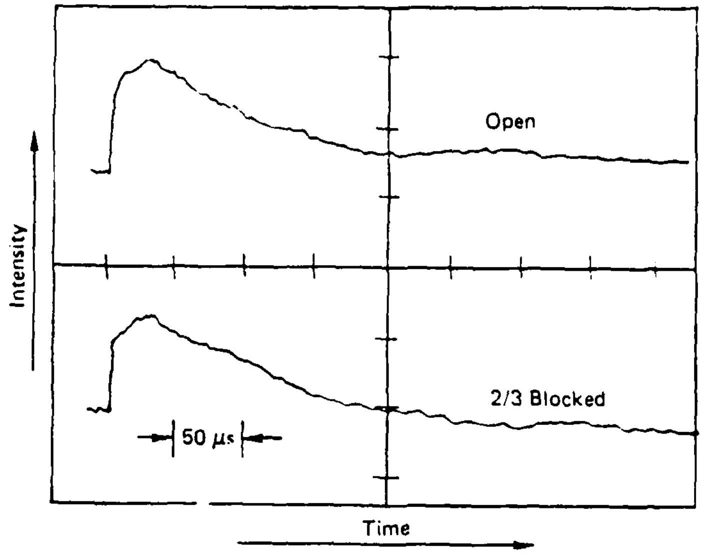

Figure 26. Nozzle Blockage Experiments. Chemiluminescent Traces Are Shown for One Experimental Condition. In Upper Trace the Operation is Normal, Whereas In Lower Trace Only 1/3 of Nozzle Length is Unblocked. The Cavity Pressure Was 22 torr

TABLE VIII. COLD REACTION NOZZLE BLOCKING EXPERIMENTS

Nozzle Arrangement	Shrouds	Peak Power (Watts)
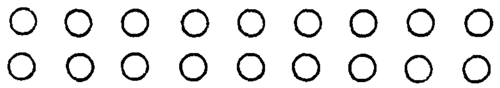	In Place	3.5
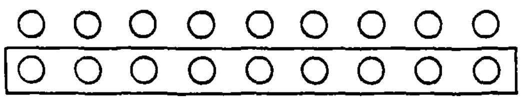	In Place	2.0
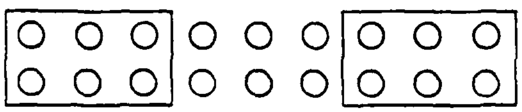	In Place	0.9
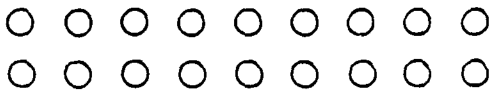	Removed	480.0

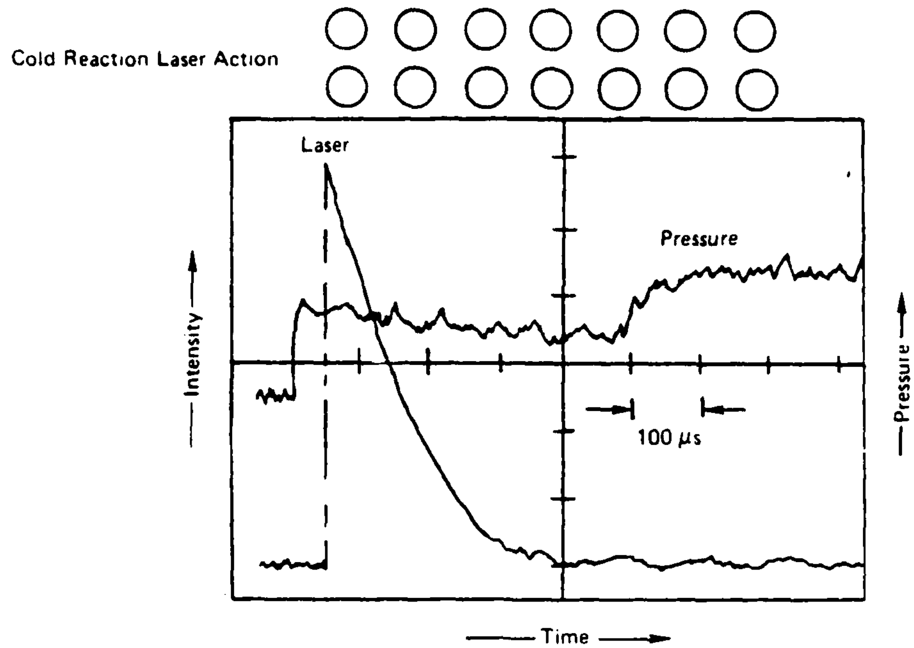

Figure 27. Laser Action at 2.7 μm Produced by the HF Cold Reaction: $F + H_2 = HF(v) + H$. The F Atoms Were Produced By Shock Heating Ar/SF_6 Mixes (2%) To Reflected Shock Conditions of 3450 K and 3.2 Atm In the 12-Inch System. Gaseous H_2 Was Injected Through the Secondary Nozzles. All Nozzles Were Clear

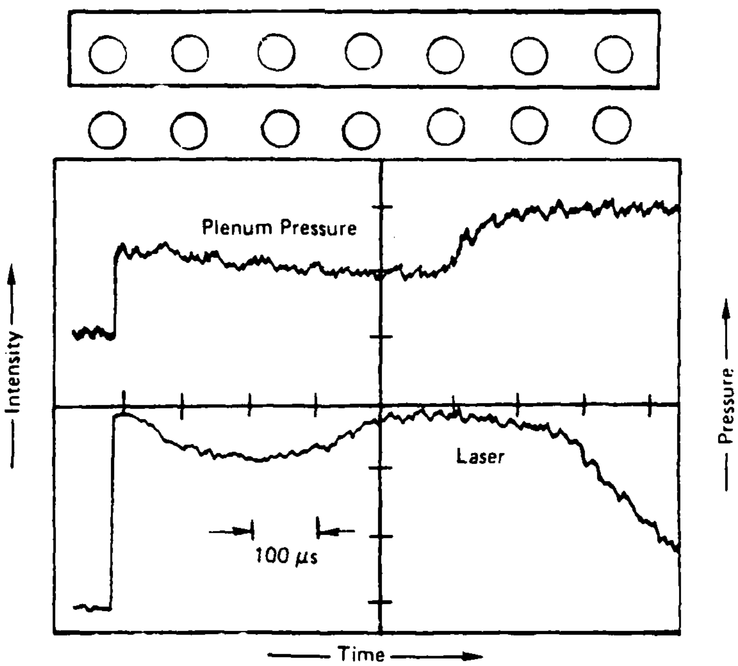

Figure 28. Nozzle Blocking Experiment With HF Cold Reaction Laser In the 12-Inch System. The F-Atoms Were Produced By Shock Heating of SF_6/Ar Mix. Upper Row of Primary Nozzle Blocked

apparent in these results. When one entire row of nozzles is blocked, the laser signal loses its transitory form and becomes very much like that of the small 3-in. nozzle which was constructed with only one row, see Figure 4 and 17. This suggests that at least for the cold reaction the transitory nature of the signal is due principally to the interaction of the supersonic effluent streams from the two nozzle rows. That this is not the case for the corresponding hot reaction is seen from the results given in Figure 16. It will be shown later that this difference can be explained on the basis of an examination of the nozzle start-up transients. The second feature of interest is that when the shrouds are removed subjecting the nozzle effluent to an additional expansion (step-function) of a factor of 2, the laser power increases dramatically. Thus, 480 W were observed from the HF cold reaction, whereas a computational analysis with the BLAZE II computer code and with the kinetics package for the H_2-F_2 system given by Cohen et al[18] gives an estimate of 640 watts for these same conditions. The BLAZE II computer code with its mixing and kinetic routines is described elsewhere.[27]

For diagnostic purposes relative to a more complete understanding of the operational characteristics of the apparatus, attempts were made to optimize the laser action derived from the cold reaction of the H_2-F_2 chemical system. A similar series of experiments for the corresponding hot reaction will be described later. Binary mixes of 2% SF_6 in argon were shock-heated to a condition of near complete dissociation. The gases were then expanded through the nozzle and varying amounts of H_2 were injected into the flow by means of the secondary nozzle array. The results are tabulated in Table IX. The cold reaction exhibits a simple exponential decay in laser intensity, see Figure 27. Thus, from a measurement of the total integrated power emitted from a given region, it was a simple matter to obtain an estimate for the peak power. The maximum power observed was for an H_2/F ratio of 16. This was the maximum reagent ratio achievable with the apparatus as now configured. It would seem that even better performance would result if higher reagent ratios could be obtained, indicating that additional expansion and high dilution levels are required to accommodate the heat release of the chemical reaction and vibrational relaxation which occur within the laser cavity. The greater heat release of the HF hot chemical relaxation will make these requirements even more severe. The exothermicity of reaction (H + HI) is nearly identical to that of the HF cold reaction, making it likely that the two systems will be somewhat similar with regard to these thermal

TABLE IX. POWER MEASUREMENTS[a] FOR THE HF COLD REACTION

Plenum Conditions T K	P (atm)	Shrouds	Γ_{H_2}/Γ_F [b]	P(watts) [c]
2700	2.3	In Place	0.23	4.4
1970	1.7	In Place	0.81	4.9
2190	1.6	In Place	1.7	2.4
2450	1.7	Removed	2.0	1.4
3350	1.9	Removed	3.4	15
3195	1.8	Removed	7	55
3310	1.9	Removed	16	474

[a] The output coupler was a flat with 20% output coupling. The total reflector had a radius of curvature of 4 m.
[b] Atomic fluorine
[c] Measured 2 cm downstream of the exit plane with 1-in. diameter mirrors (peak power).

[27] L.H. Sentman, M. Subbiah, S.W. Zelazny, "BLAZE II: A Chemical Laser Simulation Computer Program," Tech. Rpt. H-CR-77-8, MIRADCOM, Feb. 1977.

effects. This conjecture was confirmed in an effort to optimize the chemiluminescent intensity from $I(^2P_{1/2})$ at 1.3 μm, see Figure 29. Here again, the optimum performance seems to be beyond capabilities of the apparatus as far as the secondary flow rate is concerned.

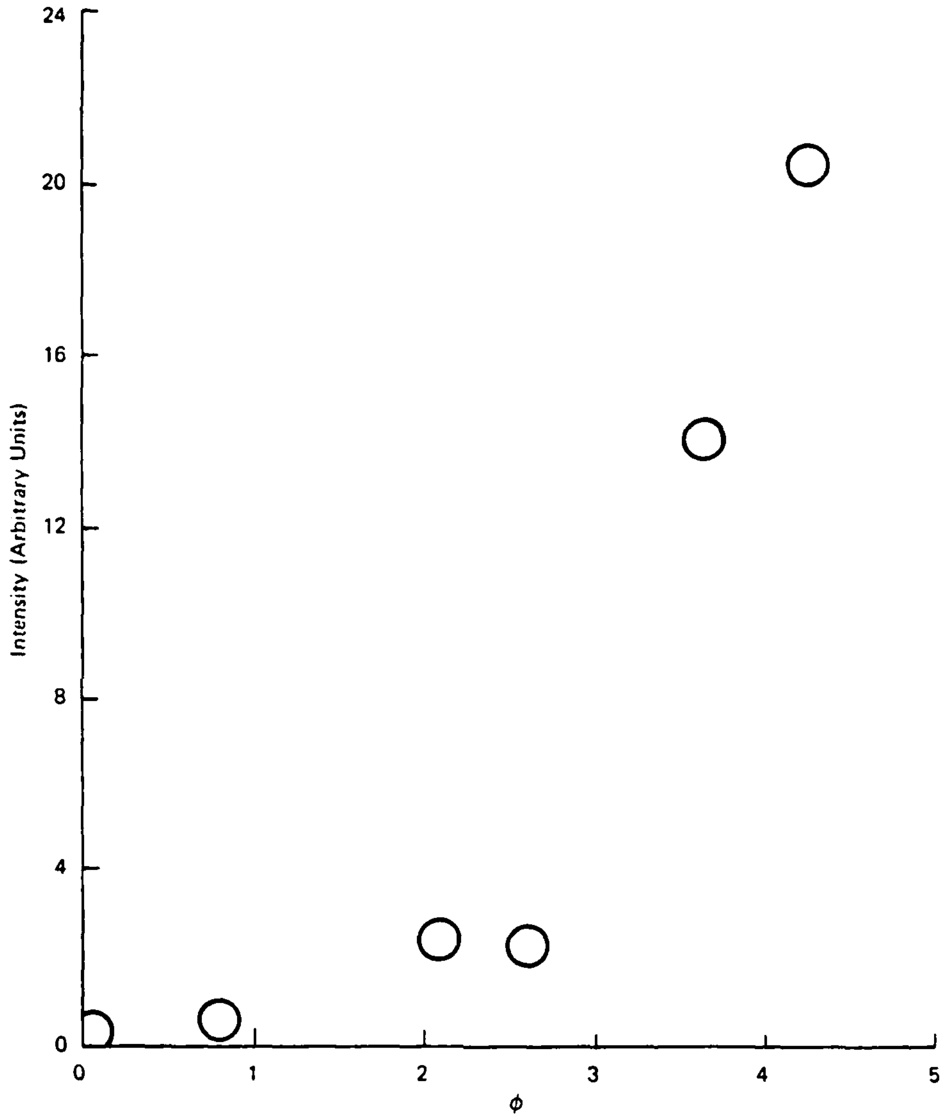

Figure 29. Illustration of the Effect of Molar Flow Ratio $\theta = \dot{n}_{HI}/\dot{n}_H$, for One Experimental Plenum Condition: 5.8% Atomic H in Ar at 3800 ±100 K and 3.2 ±2 Atm

It was suggested above that the explanation of the transitory nature of the radiant intensity levels emanating from HF hot reaction laser action within the laser cavity could be explained, at least in part, on the basis of the start-up transients to be expected for the nozzle configuration used. The analysis used here has been described in detail by Rudinger.[25] For explanatory purposes, a typical wave diagram is illustrated in Figure 30. Typically, for experiments of the type under consideration, the unshocked gas within the shock tube, Region 1, will be at 300 K and 10-20 torr and will have a

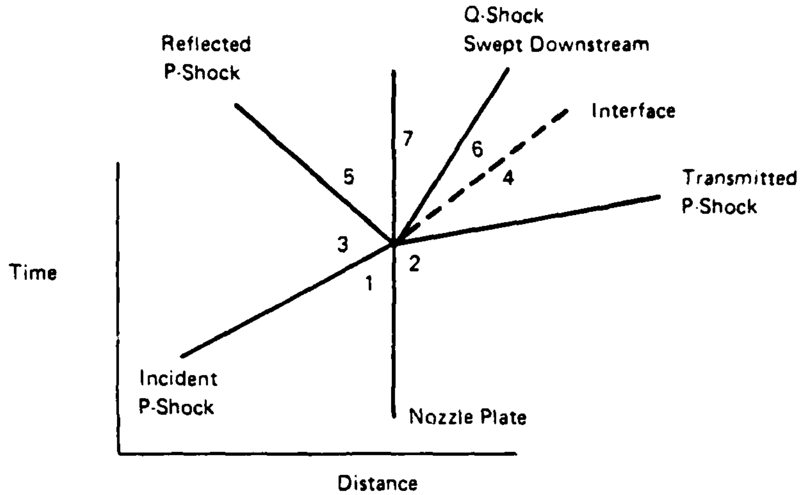

Figure 30. Typical Wave Diagram

composition consisting of 3% H_2 in argon. The gas behind the incident shock wave, Region 3, will be at approximately 2200 K and 0.5-1.0 atm and will have the same composition. After shock reflection from the nozzle plate, the gas, Region 5, will have a temperature in excess of 4000 K, a pressure in the neighborhood of 3 atm, and will consist of a mixture of 5.8% atomic hydrogen in argon. The gas isentropically expands from Region 5 into Region 7 where its temperature and pressure are in the ranges of 300 K and 2-3 torr respectively. At the same time, a shock wave is transmitted through the nozzle into the undisturbed gas initially in Region 2 and a new region of high temperature gas, Region 4, is created. The gas in Region 4 will have a temperature and pressure which depend upon the degree of mixing of unshocked primary and secondary flows in Region 2. Typically, however, these values will be in the neighborhood of 1000 K and 80 torr respectively. Finally, in order to balance the dynamic variables in Regions 7 and 4, a new backward facing, Q-shock is created which is slowly swept downstream by the high velocity gas in Region 7. This Q-shock creates a new region of high temperature gas, Region 6, which will have a temperature in the neighborhood of 4000 K and a pressure of about 80 torr. Regions 4 and 6 are separated by an entropy interface which separates the gases that were initially in Regions 2 and 1 respectively. These estimates assume that no expansion occurs beyond the exit plane of the nozzle. If a step function is present, allowing a further expansion area ratio of 2, the temperatures and pressures in Regions 4, 6, and 7 will tend to somewhat lower values. The actual wave diagram for one experimental condition is shown in Figure 31. Only the conditions in Regions 2, 4, 6 and 7 are depicted as the conditions in Region 5 are given separately.

A simple explanation of the transitory nature of the hot reaction signal can now be offered. Passage of the transmitted P-shock through the mixed gases in Region 2 will cause considerable dissociation of the F_2 present. This will initiate cold reaction laser action, although the high pressure will assure poor efficiency. Passage of the diffuse interface introduces another high temperature region causing total dissociation of all F_2 present. This will cause a considerable drop in temperature permitting cold reaction laser action to continue in an inefficient manner. Passage of the Q-shock at about 250 μs (2 cm downstream) introduces a new region of low temperature, low pressure gas of the proper composition for hot reaction laser action. Unfortunately, the temperature and pressure in

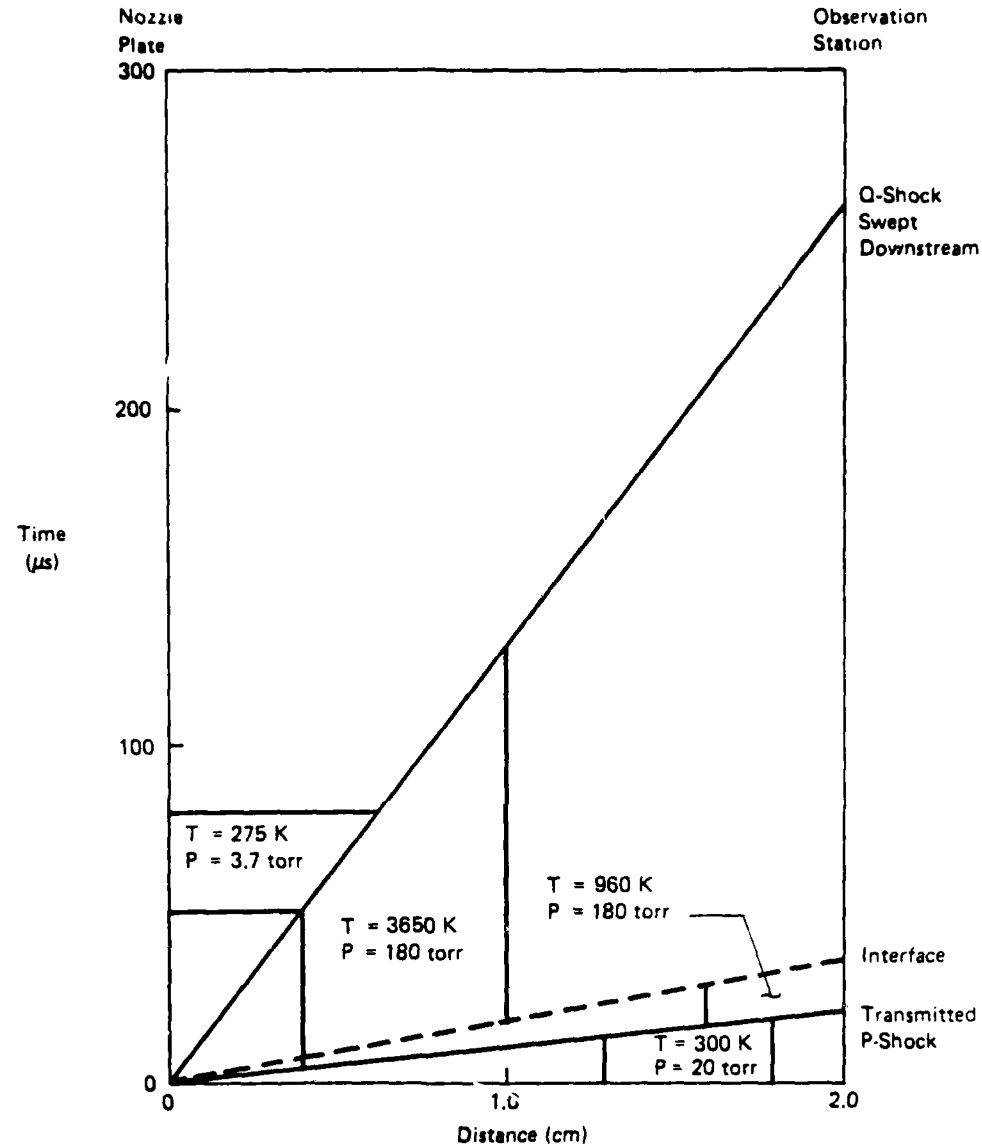

Figure 31. Wave Diagram for One Hot Reaction Experimental Condition. The Plenum Temperature and Pressure Were 4200 K and 4.4 Atm. Resp. With X_{Ar}: X_H = 89:11. Initial Gas Composition Was 6% H_2 In Argon at 20 torr and 300 K. The Shock Velocity Was 1.6725 mm/μs. The Area Ratio Was 20. See Fig. 33.

this region are far from optimal and laser action ceases. Of course, from the nozzle blocking experiments, Figures 27 and 28, we must conclude that interaction of the effluent streams from the two rows of primary nozzles is also of importance here, although this effect has been neglected in construction of the wave diagram.

When one row of primary nozzles is blocked, the cold reaction produces steady laser action, see Figures 17 and 28. This effect can also be explained on the basis of the wave diagrams. Thus, at 24 μs, the P shock passes the window exposing a gas region having a temperature of about 900 K and a pressure of 83 torr. The high temperature dissociates some of the fluorine present and cold reaction laser action begins. Passage of the interface causes total dissociation of the fluorine and laser action continues. Passage of the Q-shock leaves a near optimal condition for cold reaction laser action. Laser action continues until the arrival of the contact surface or the rarefaction at the nozzle plate abruptly changes the plenum conditions.

The nozzle was originally configured to an area ratio of 20. Although this is satisfactory for the production of fluorine atoms, see Figure 32, it leaves much to be desired in the case of hydrogen atom production, Figure 31. Accordingly, late in the program the area ratio was changed

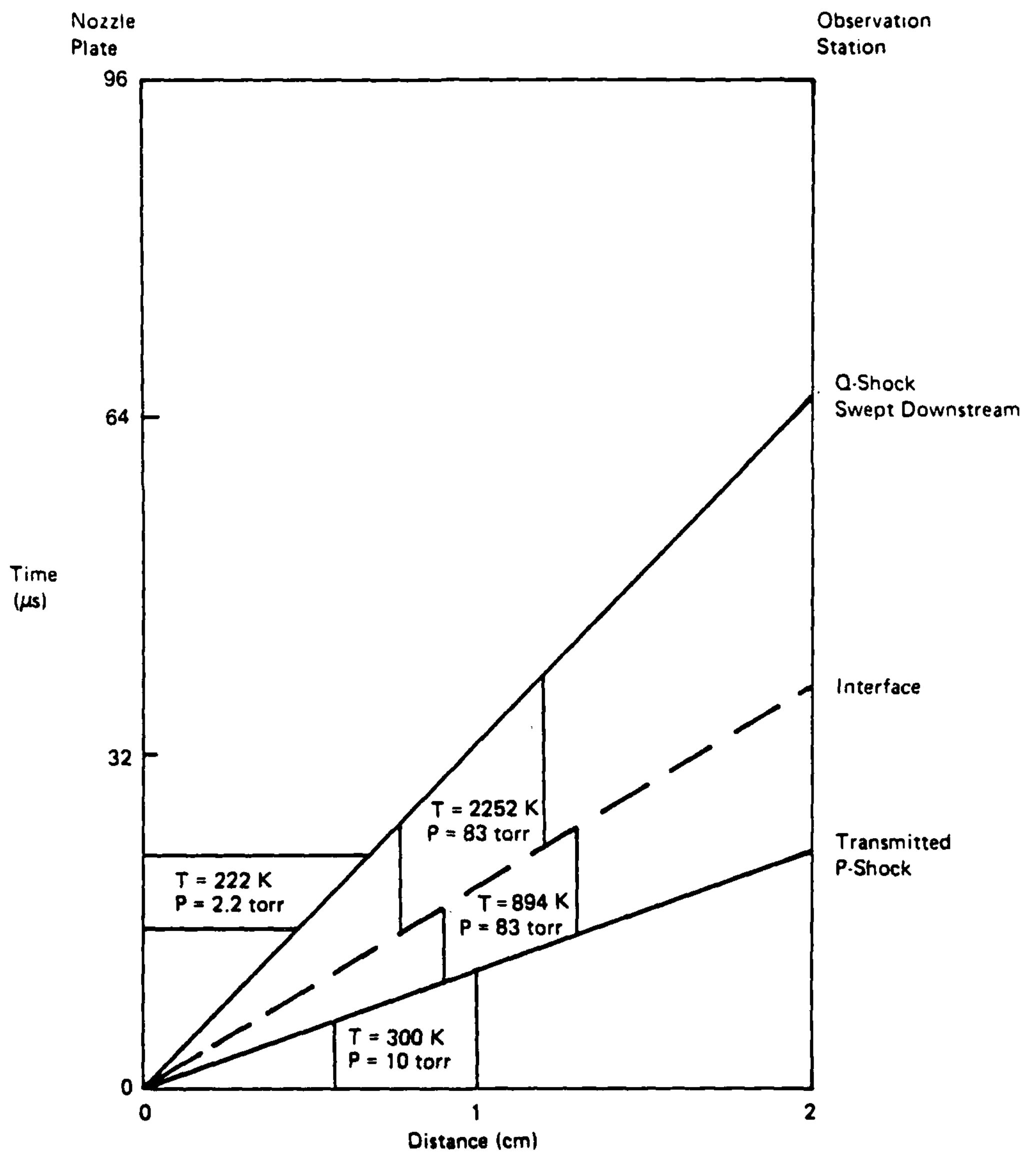

Figure 32. Wave Diagram for One Cold Reaction Experimental Condition. The Plenum Temperature and Pressure Were 3385 K and 2.7 Atm. The Initial Gas Composition Was 2% SF_6 In Argon. The Area Ratio Was 20

to 11. A typical wave diagram for this configuration is shown in Figures 33-34. There are two striking differences produced in the wave diagram on going to a smaller area ratio. First, the time required for passage of the backward facing Q-shock is considerably shortened, see Figure 31, and secondly, the pressure in Region 7 is greatly increased. The latter factor would seem to insure a more optimal condition for the HF hot reaction. Indeed, a new region of laser action is to be expected following an initial burst from the cold reaction chemistry as discussed previously. A typical oscillogram showing the operation of the hot reaction chemistry is given in Figure 35. It would seem probable at this point that the steady decline in laser power and cavity pressure, as shown in this figure, is due principally to the shock interaction between the two rows (levels) of nozzle effluents as discussed previously in connection with the blocking experiments. Several experiments were conducted at variable Γ_{F_2}/Γ_H ratio in a search for optimal operating conditions. Unfortunately, due to several safety restrictions with regard to the handling of F_2, it was not possible to obtain very high values for this ratio. The results are given in Table X.

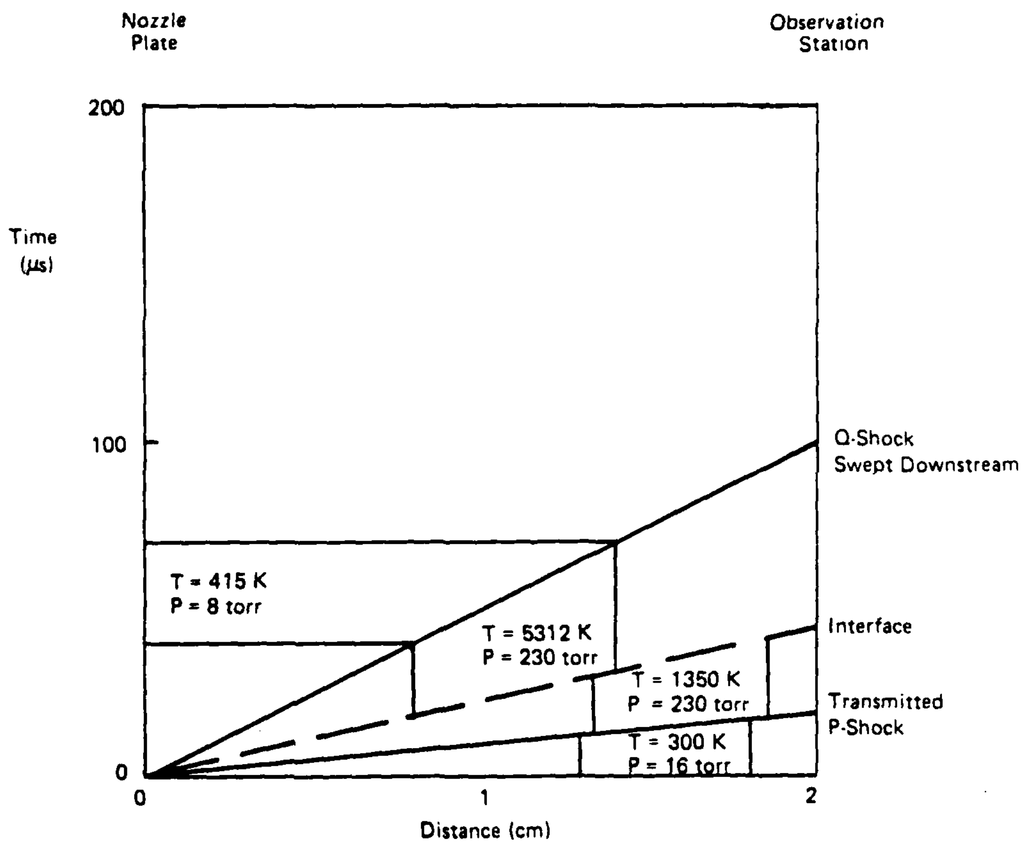

Figure 33. Wave Diagram for One Hot Reaction Experimental Condition. The Plenum Temperature and Pressure Were 4200 K and 3.5 Atm. Resp. With X_{Ar}: X_H = 89:11. Initial Composition Was 6% H_2 in Ar at 20 torr and 300 K. The Shock Velocity Was 1.6725 mm/μs and the Area Ratio Was 11. See Fig. 31

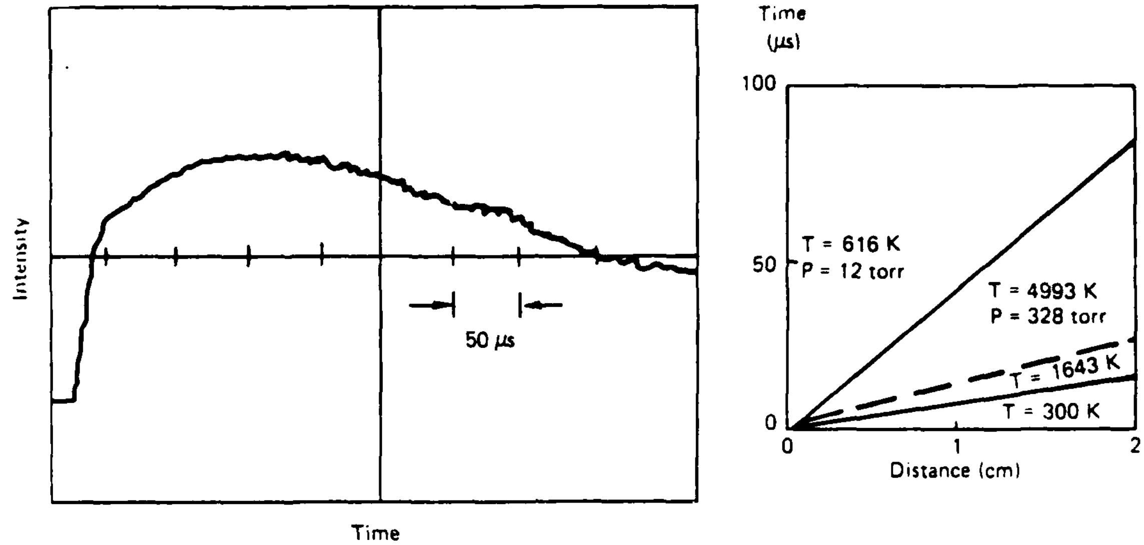

Figure 34. Chemiluminescence From Atomic Iodine at 1.3 μm. The 12-Inch System Was Used with a Nozzle Area Ratio of 11. Plenum Conditions Were 6230 K and 5.1 Atm. With $X_H \sim 0.058$. Gaseous HI Injected Into Flow With θ (HI/H) ~ 1.6. Observation 2.0 cm Downstream of Exit Plane

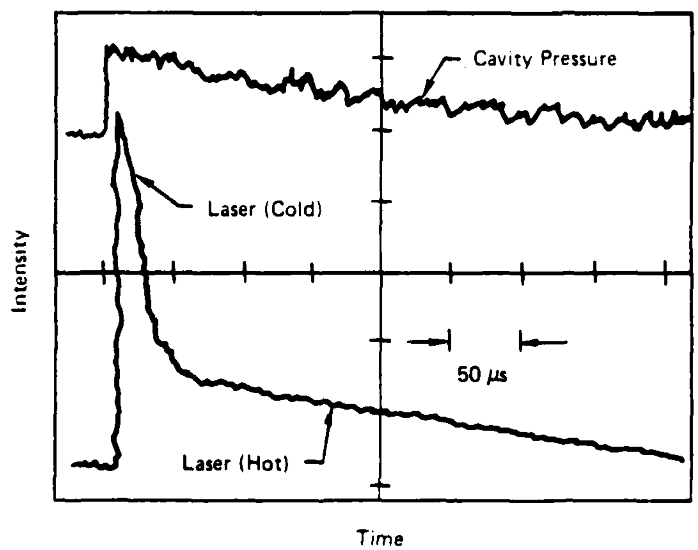

Figure 35. Laser Action at 2.7 μm Derived from HF. The Plenum Was 11% Atomic H in Ar at 4200 K and 3.5 Atm., $\Gamma_{F_2}/\Gamma_H \sim 0.34$. Peak Cavity Pressure Measured at ~ 9 torr

TABLE X. POWER MEASUREMENTS [a] FOR THE HF HOT REACTION

Plenum Conditions				mol/s				
%H	T K	P (atm)	Shrouds	Γ_{F_2}	Γ_H	Γ_{F_2}/Γ_H	P (Watts) [b]	A_R/A_L
5.8	3400	2.7	In Place	0.008	0.031	0.25	1.7	20
5.8	4020	2.8	In Place	0.050	0.029	1.7	1.8	20
5.8	3630	2.4	Removed	0.024	0.026	0.9	4.9	20
5.8	3460	2.8	Removed	0.030	0.033	0.9	4.4	20
5.8	4670	4.2	Removed	0.042	0.041	1.0	4.4	20
5.8	3470	2.4	Removed	0.022	0.027	0.8	5.2	20
5.8	3410	2.0	Removed	0.027	0.040	0.7	3.5	11
11.3	4200	3.5	Removed	0.045	0.131	0.3	3.5	11
11.3	5860	2.0	Removed	0.031	0.034	0.9	3.5	11
21.4	4600	2.2	Removed	0.022	0.080	0.3	3.9	11
21.4	3800	4.6	Removed	0.027	0.181	0.15	3.5	11

[a] The output coupling was by means of a 0.5-mm-diameter hole. The total reflector had a radius of curvature of 4 m. Both mirrors were 1 in. in diameter.

[b] Peak power (after initial transient for $A_R/A_L = 11$).

Calculations of expected laser power with the BLAZE II [27] computer code, based upon the kinetics package for the H_2-F_2 system as compiled by Cohen,[18] gives values in the neighborhood of 2 kW for conditions similar to those given in Table X. This suggests strongly that most of the atomic hydrogen that should exist in Region 7 of the wave diagram, see Figures 31, 33, has been converted to the corresponding molecular form on passage through the nozzle. This, a major conclusion with regard to these studies, was partially confirmed in the early stages of the program. Thus, for the 3-in. system a nozzle was constructed of plexiglass and tested. The luminescent intensity at 1.3 μm was enhanced by approximately a factor of 3 over that observed for an identical nozzle constructed of stainless steel, see Table IV(a). Similarly, slot nozzles constructed of nylon were tested and found to give good performance, see Table IV(b).

A very simple calculation procedure can be used to estimate the extent of hydrogen atom recombination on the nozzle surfaces during transit into the reaction chamber. We compute the diffusional rate of hydrogen atoms through a thin cooled gaseous film to the surface. Mirels[28] has given a thorough analysis of boundary layer growth in shock-tubes which can be used directly here. For a nominal plenum condition corresponding to 4000 K at 2.6 atm with $X_H \sim 0.058$, it can be shown that the boundary thickness in Region 3 is given very approximately by the following expression:

$$\delta_3 \sim 3.7\sqrt{\frac{\nu_3(u_s\,\tau - \xi)}{u_s}} \tag{18}$$

A similar expression is needed for the gas in Region 5.

28 H. Mirels, "Attenuation In A Shock-Tube Due To Unsteady Boundary-Layer Action," NACA Report 1333, 1957.

When the shock reflects from the tube end and propagates back upstream, it produces a stagnant core of test gas. The reflected shock also interacts with the wall boundary layer produced in Region 3. Depending on the specific heat ratio, this shock wave – boundary layer interaction can result in a Lambda type shock and flow separation. Based on criteria established in Reference 29, this will not occur here.

Based on the above, it will be assumed that δ_3 will provide a good estimate of the extent of the boundary layer influence. With thermodynamic and transport properties calculated for the test case, and assuming a 750 μs test time, a maximum boundary layer thickness of 2 mm is predicted. This value is over an order of magnitude smaller than that required for the wall boundary layer to have a significant effect upon the test results. It would appear that the boundary layer influence is negligible.

The nozzle block contains 190 individual nozzles with an active exit area of 31 cm^2. The primary throats were altered late in the program to a diameter of 0.103 cm and have a total area of 1.58 cm^2. The subsonic portion of the assembly has a surface area of 76 cm^2 exposed to the oncoming gas. In the reflected shock region, the nominal gas conditions are those given above. This results in a total flow rate of 32 g for the argon-hydrogen mixture. With this date, it is straightforward to calculate the usual gas dynamic properties. Thus, the approach Mach number is 0.002, the sound velocity in Region 5 is 1195 m/s, and the mean flow velocity, V_5, of gas moving toward the nozzle inlet is (1195) x 0.002) or 2.9 m/s.

We estimate the particle residence time in the nozzle by assuming a linear velocity increase. The nozzle is 0.32 in. long. For given areas and γ, the exit Mach number will be in the vicinity of 5.3. The cavity temperature will then be 400 K and the exit plane velocity will be 1975 m/s. Since the velocity at any given point within the nozzle is given by

$$V = F_5 + (V_e - V_5)\frac{x}{0.32} \qquad (19)$$

the passage time will be given by

$$\Delta t = \int_0^{0.32} \frac{dx}{V_5 + (V_e - V_5)\frac{x}{0.32}} = 27\ \mu s \qquad (20)$$

It is also of interest to see how much gas is taken from Region 5 during a test run. With a flow rate of 32 g/s for 750 μs, a total of 0.024 g of the plenum mixture passes through the nozzle. In region 5, the gas density is 0.0031 g/cm^3. With a plenum cross-sectional area of 200 cm^2, a slug of gas of thickness ΔL = 0.038 cm will flow through the nozzle. This is admittedly a very simplified picture, but it does help in formulating some of the remaining calculations.

29. S. Byron and N. Rott, "On the Interaction of the Reflected Shock Wave with the Laminar Boundary on the Shock-Tube Walls," Proceedings of the 1961 Heat Transfer and Fluid Mechanics Institute, Stanford, Calif., 1961, p.38.

Based upon the results to this point, it is now possible to examine the heterogeneous recombination of hydrogen atoms on the walls of the plenum. In this calculation, we ignore lateral diffusion to the plenum walls and consider diffusion to the nozzle block itself. As stated previously, the calculation assumes diffusion by H atoms through a stagnant film with recombination at the wall to produce H_2. The H_2 is assumed not to redissociate. The model and solution are given in Reference 28 and will not be repeated in detail here. A simple sketch of the problem is given in Figure 36. The molar flux of hydrogen at the surface is given by[30]

$$\dot{N}_H = \frac{2(\frac{P}{RT})\, A^* D_{H-M}}{\delta} \ln\left(\frac{1}{1-\frac{x_H}{2}}\right) \qquad (21)$$

The subsonic channel of the nozzle has a total exposed surface area of 76 cm^2. Then, for a stagnant film thickness, as estimated above (0.038 cm), there results for $D_{H-M} \sim 890\ cm^2/s$

$$\dot{N}_H \sim 0.035 \text{ mol/s}$$

This represents the loss of H atoms to the wall of the subsonic channel of the right nozzle block assembly. The nozzle flows 32 g/s of plenum fluid or 0.049 mol/s of atomic hydrogen. Hence, of the total molar flow rate of atomic hydrogen, up to 70% is lost to recombination on the nozzle block face.

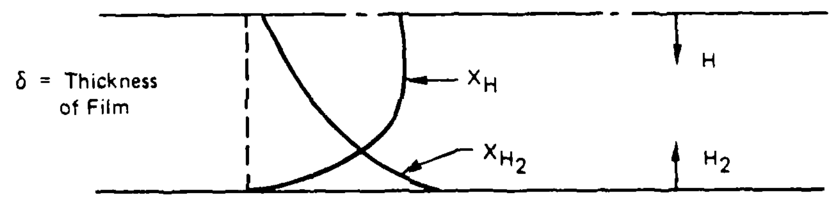

Figure 36. Sketch of Diffusional Problem for Recombination of Hydrogen Atoms on the Walls of the Nozzle Block Assembly

A crude estimate of the recombination losses within the supersonic portion of the nozzle can be obtained by replacing the stagnant film thickness used above by a characteristic nozzle half width. Doing this results in a recombination loss of up to 10%. In conclusion, based on the simple calculations done here, it appears that about 75% of the hydrogen atoms initially present are lost to the flow by wall recombination, 70% on the subsonic side and 5% after passage through the throat.

To investigate these conclusions experimentally, the inside of the supersonic portion of the nozzle was coated with a 40 micro-inch layer of SiO_x ($1 < x < 2$). A vapor deposition technique was used. It was anticipated that the deposit would substantially change the surface characteristics giving some indication of the correctness of the conclusions reached above regarding recombinative effects. The resultant chemiluminescent pulse in comparison to the results obtained for the uncoated surface is shown in Figure 37. The results were duplicated several times and it now appears certain

30 R. B. Bird, W. E. Stewart, and E. N. Lightfoot, "Transport Phenomena," John Wiley and Sons, Inc., New York, p. 529, 1960.

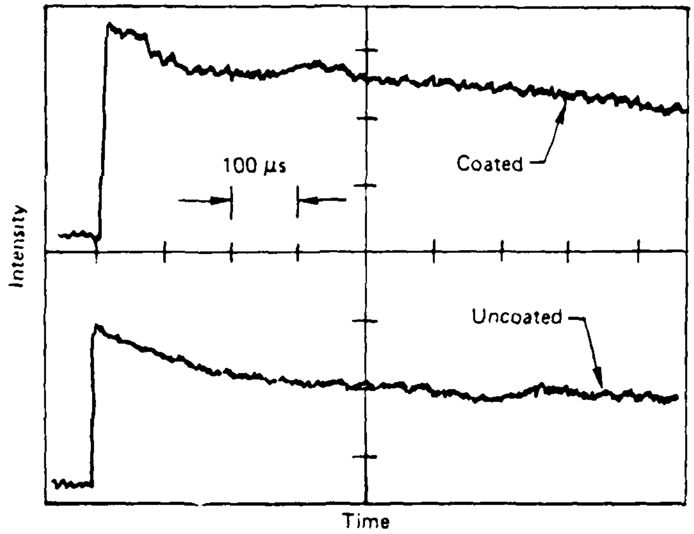

Figure 37. Chemiluminescence From Atomic Iodine at 1.3 μm. The 12-Inch System Was Used With an Area Ratio of 11. Plenum Conditions Were 4770 K and 2.6 Atm With θ(HI/H) ~ 3.4. Observation at 2.5 cm From Exit Plane For Glass Coated and Un-Coated Configurations (Supersonic Parts)

that coating the supersonic portion of the nozzle with a SiO_x substrate improves the performance of the system by about 50%. Although this is a somewhat greater effect than predicted analytically above, the comparison is qualitatively satisfactory. Time did not permit an extension of these experiments to the subsonic region of the system. Based upon these results, however, it can be anticipated that a very sizeable effect could be obtained.

Late in the experimental phase of the program, the windowed section was lengthened to permit observations at distances of up to 15 cm from the nozzle exit plane. Chemiluminescent data were taken at various axial positions downstream and the data are illustrated in Figure 38. It would appear that the intensity increases regularly with distance over the available range of the apparatus. Unfortunately, the optimal condition is beyond the range of the present apparatus. This behavior is likely, at least in part, to be due to the relatively slow nature of the transfer process, equation (8). In any actual analysis of these results, however, it would be necessary to take account of the attenuation of the flow velocity within the cavity with its attendant effects upon the gas density. A lasing demonstration was attempted with the optical axis at a distance of 13.5 cm downstream of the nozzle exit plane, see Figure 39. Although considerable resonant enhancement at 1.3154 μm was observed during the aligned cavity experiment, lasing did not occur.

Finally, a simple countoured slot nozzle was constructed for the 12-in. system after the design shown in Figure 3. Injection of HI was just downstream of the throat. The area ratio was 10 and the material of construction was aluminum. The nozzle was used to produce chemiluminescence from atomic iodine for one experimental condition. The results are illustrated in Figure 40. The results obtained are roughly comparable to those given by the nozzle array for an area ratio of 11, see Figure 38. Even the shape of the curve is somewhat similar for the two nozzles, see Figure 39. This result is in agreement with the conclusions reached earlier regarding the dependence of the start-up transients upon the nozzle area ratio. A lasing demonstration with the slot nozzle arrangement again proved unsuccessful.

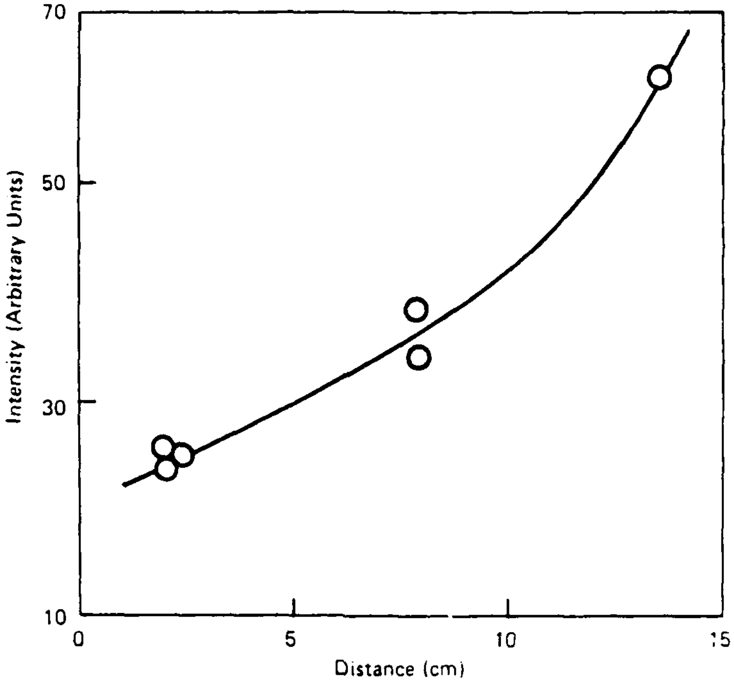

Figure 38. Illustration of the Effect of Axial Distance From Nozzle Exit Plane Up n the Chemiluminescent Intensity at 1.3 μm. Plenum Conditions Were 6300 ± 100 K and 3.2 ±0.2 Atm With θ (HI/H) ~ 3.3 ±0.3 In Cavity. The Area Ratio Was 11. The Aperture Was 0.5 x 1.0 cm^2 at the Window

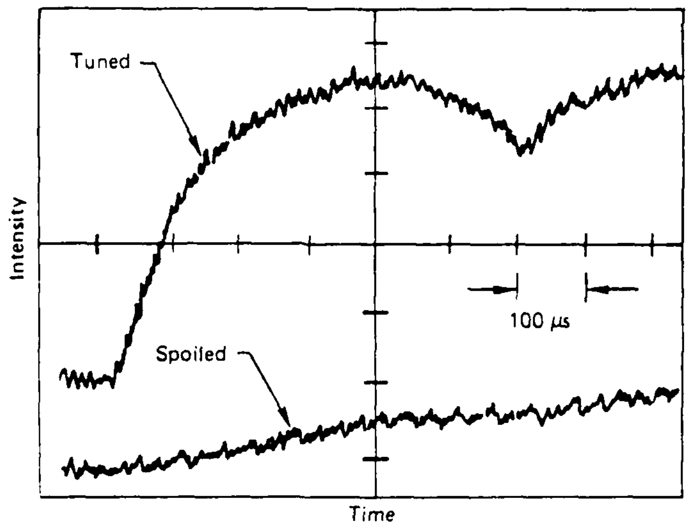

Figure 39. Illustration of Cavity Experiments for Radiation Emanating From a Position 13.5 cm From Nozzle Exit Plane. Plenum Conditions of 6430 K and 2.9 Atm. With θ (HI H) ~ 3.3. The Area Ratio Was 11

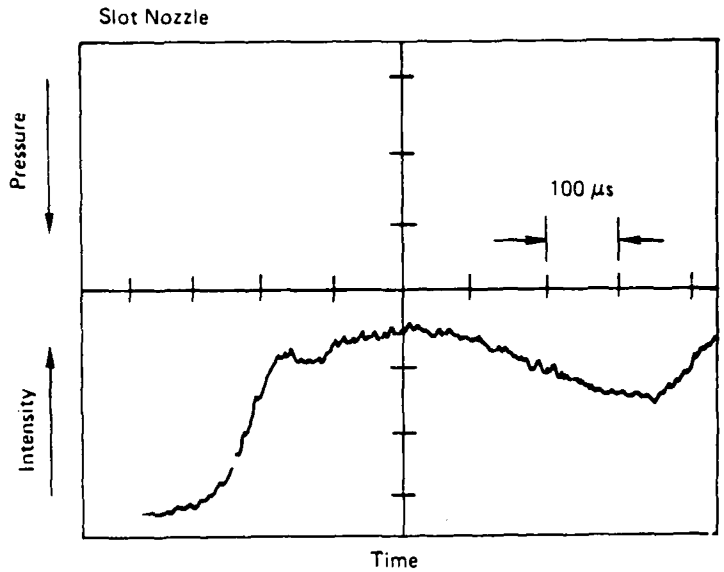

Figure 40. Chemiluminescence From Atomic Iodine at 1.3 μm. The 12-Inch System Was Used With a Simple Contoured Slot Nozzle Having an Area Ratio of 10. Plenum Conditions Were 5800 K and 3.4 Atm. With $X_H \sim 0.058$. Gaseous HI Injected Into Flow With θ (HI/H) ~ 2.4. Observation Was 13.5 cm Downstream of Exit Plane

IV. DOUBLE RESONANCE GAIN MEASUREMENTS IN A SUBSONIC FLOW TUBE (PHASE III)

The previously described experimental work centered around shock heating hydrogen gas to generate the necessary atomic hydrogen reactant. The task undertaken in this part of the program was to examine a system which would generate the hydrogen atoms in situ with HI and ultimately demonstrate gain.

It has long been known that alkali metal atoms react with hydrogen halide molecules in the gas phase with a bimolecular rate constant which may exceed collision frequency[31, 32]. The product of such an encounter is typically a hydrogen atom and a metal halide molecule. Rate data for several reactions involving HI have been reported and tabulated in Table XI.

TABLE XI. REACTION RATE DATA FOR GAS PHASE ENCOUNTERS BETWEEN ALKALI METAL ATOMS AND HYDROGEN IODIDE

Reaction	T K	k (cm^3/molec·s)
Li+HI = LiI+H	300 - 350 K	1.36×10^{-9} (est.)
Na+HI = NaI+H	300 - 350 K	8.33×10^{-10}
K+HI = KI+H	300 - 350 K	3.31×10^{-9}

The system thus chosen involves the following chemistry:

$$M + HI = MI + H$$

$$H + HI = H_2(v \leq 3) + I(^2P_{3/2})$$

$$H_2(v \geq 2) + I(^2P_{3/2}) = H_2(v-2) + I(^2P_{1/2})$$

Sodium was somewhat arbitrarily chosen as the reactant candidate in which these experiments would be carried out.

1. EXPERIMENTS

The experiment basically involves vaporizing sodium, flowing it with a carrier gas through a nozzle and injecting HI + diluent at the nozzle exit plane. Downstream of this (optical zone) demonstration of gain (or loss) would be accomplished employing the double resonance technique developed by Benard[33] which is sufficiently sensitive for making gain measurements over the short gain lengths. Schematic views of the arrangement are shown in Figures 41 and 42.

The sodium oven consists of a 5 inch diameter stainless tube 6 inches long and sealed at both ends. Several turns of quarter inch stainless tubing are wound around the cylinder, one end of which feeds into the cylinder. The unit is surrounded by two semicylindrical heating elements. In this way helium flowing through the tubing is preheated and injected into the oven containing sodium

31. H. Schay, Z. Phys. Chem., 11 B, 291 (1930)
32. M. Polanyi, "Atomic Reactions," William and Norgate Co., London (1932).
33. A. T. Pritt et al, Appl. Phys. Lett. 31, 745 (1977).

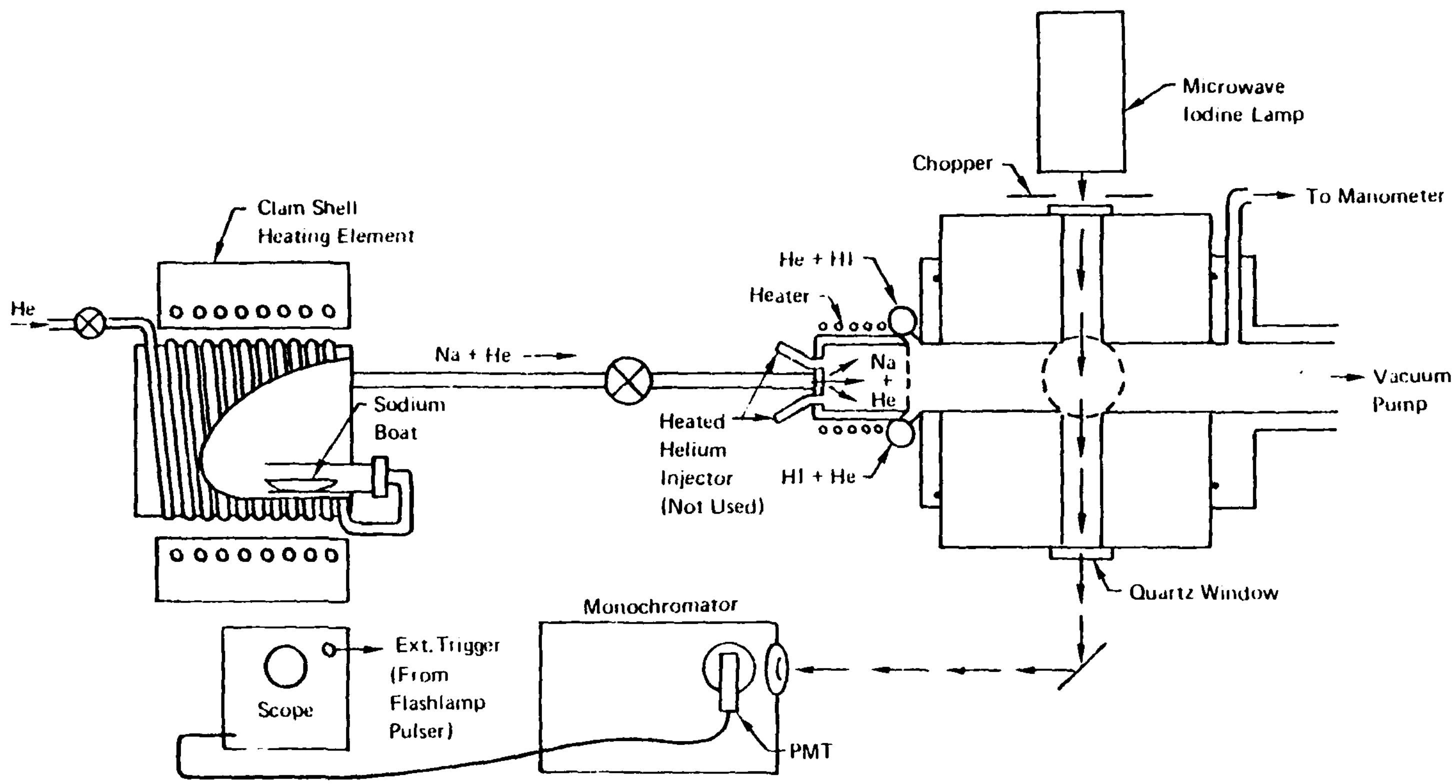

Figure 41. Side View of Experimental Arrangement

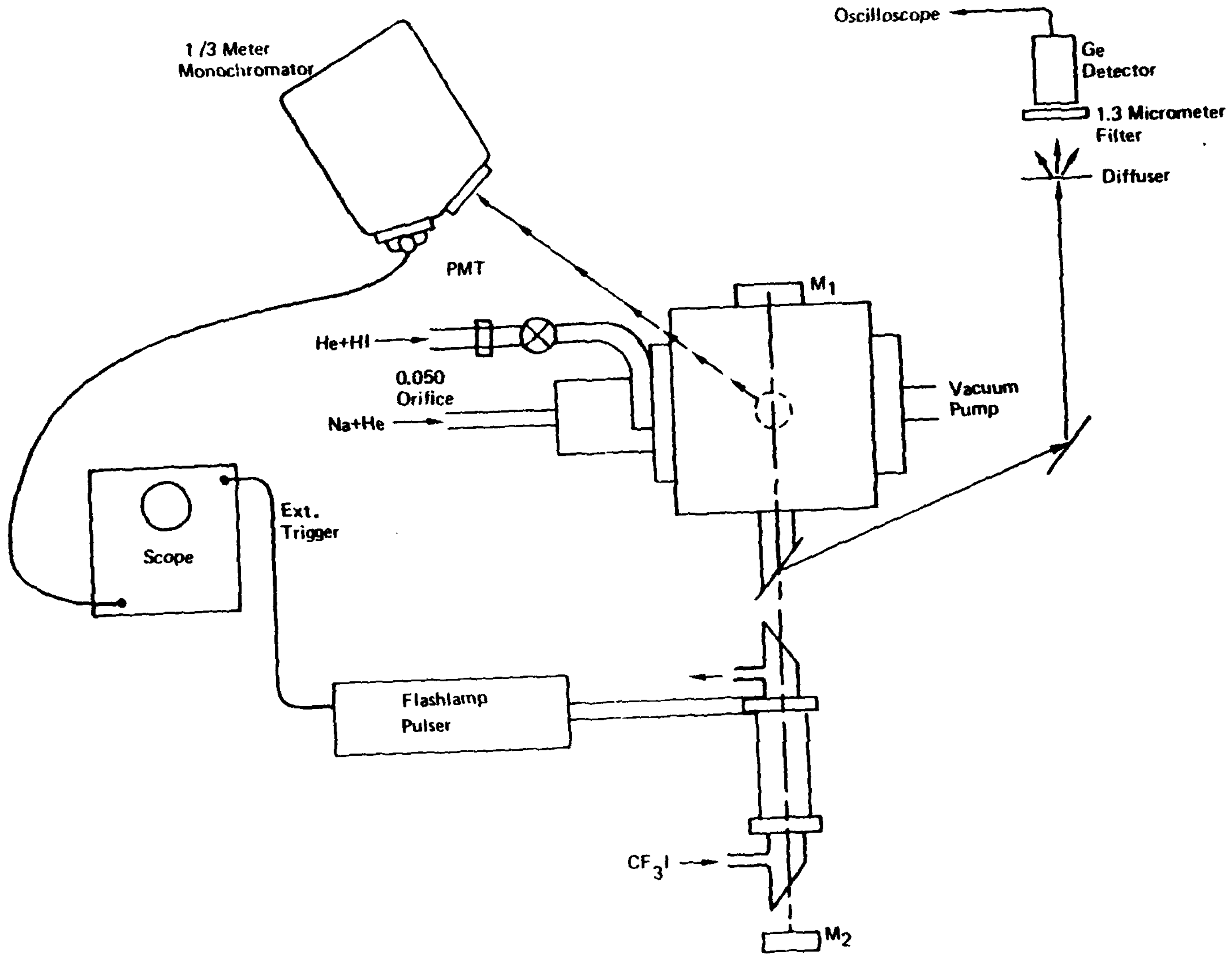

Figure 42. Top View of Experimental Arrangement

and acts as a carrier gas for flowing sodium into the nozzle. The oven temperature is routinely maintained around 600-650 C.

Originally the sodium vapor and preheated helium were to be independently flowed into a heated premix chamber and then injected sonically into the optical cavity through a series of eight slots. One-third of the total helium was to be flowed in this manner. This concept was arrived at so as to alleviate certain practical problems envisioned with narrower slots if sodium was flowed alone. The premix chamber with slot injector has a diameter of 1 in. This matches the flow tube diameter which it feeds. On the flow tube side of the slots a mixture of helium and HI is injected from above and below through slots measuring 0.215 in. wide by 0.834 in. long.

At first it was found that sodium and HI were reacting too far upstream, probably in the premix chamber. In addition the sodium appeared to be clogging the 0.046-in. diameter orifice through which sodium enters the chamber. These problems were resolved by directing the preheated helium into the sodium oven and utilizing the 0.046-in. orifice as a sonic orifice to control the helium flow rate.

The flow tube/optical cavity was loaned to BAT by the Air Force Weapons Lab. It is a 4 x 4 x 4-in. aluminum block with three mutually perpendicular holes bored through and intersecting at the center of the block. One bore, the flow tube channel, was 1 in. in diameter, and the other two are about one centimeter in diameter.

Radiation from a cw microwave iodine lamp passes through a quartz window located on the top of the block and exits through another quartz window on the bottom. The radiation is then reflected by a mirror directing it to a 1/3 meter monochromator set to detect 2062 Å radiation.

The remaining channel is an integral part of the pulsed iodine laser. A high reflectance (at 1.315 μm) dielectric mirror (M_1) having a 2-m radius of curvature is O-ring sealed to the block. The opposite end of this channel is sealed off with a Pyrex Brewster window (uv blocking). Aligned along the optical axis of this combination is a Candela CL-1000 cylindrical flashlamp advertised as capable of handling 1000 joules for about 5000 shots. The ends of the flashlamp were fitted with BK-7 crown glass Brewster windows. Forty torr of CF_3I was flash photolyzed inside the lamp. A high reflectivity flat mirror (M_2) completes the pulsed iodine laser resonator.

Reflections from the flow tube Brewster window directed toward a Ge detector/1.3μ filter was used to verify laser operation during tests. The changes in absorbance of the 2062 Å radiation detected by the PMT were observed on an oscilloscope triggered by a flashlamp discharge sensor.

The flashlamp pulser consists of two 2 μF capacitors (in parallel) typically charged to 20 kV. The iodine laser pulse shape is reproduced in Figure 43.

Typical flow rates of the component gases were calculated to be

HI = 3×10^{-3} mol/s

He (from oven) = 3.5×10^{-2} mol/s

He (in HI) = 2.7×10^{-2} mol/s

Na (est) = 3.5×10^{-4} mol/s

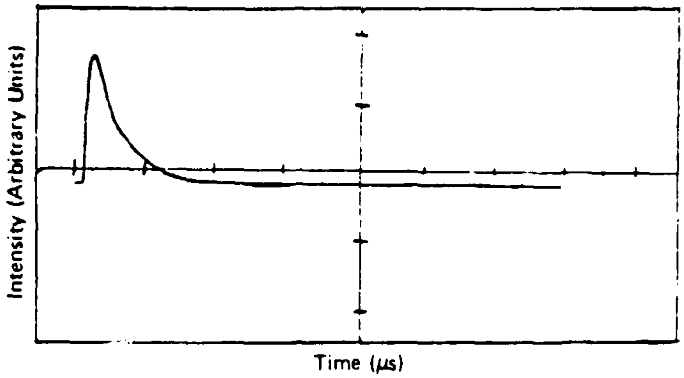

Figure 43. 1.315 μm Iodine Laser Pulse. Sweep Rate - 10 μs/Div. 40 Torr CF_3I

Although the temperature in the optical cavity was not measured the Mach number was estimated to be 0.25. This was calculated using the measured pressure (~ 18 torr) and assuming 450 K gas temperature and a molecular weight of about 9.6.

The flow tube with the double resonance gain measurement apparatus in place is shown in Figure 44.

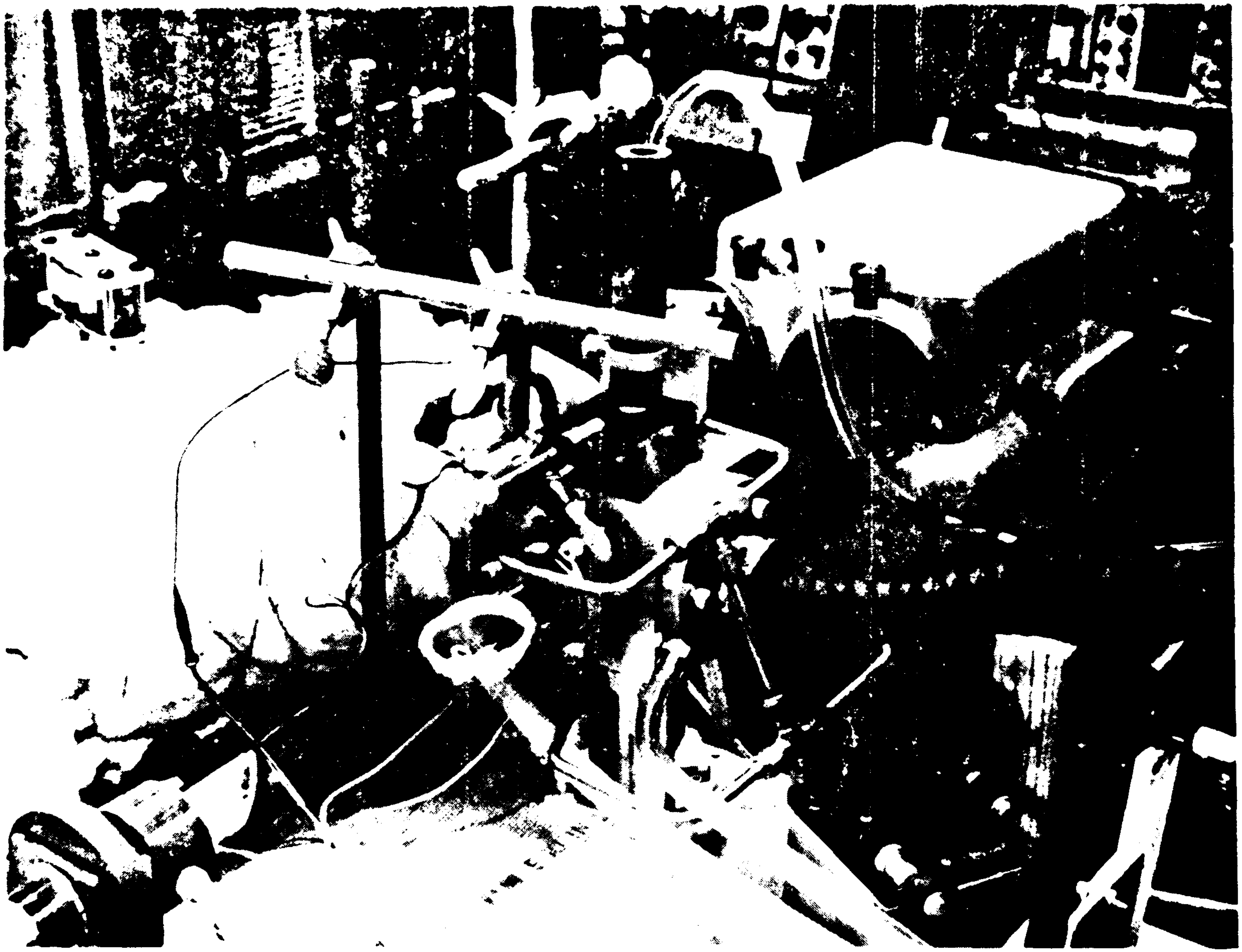

Figure 44. Photograph of the Double Resonance Apparatus - Viewing the Flow Tube

2. RESULTS

To verify the presence of atomic iodine in the optical cavity an absorption experiment was performed on the 1830 Å line. This line has an order of magnitude larger absorption coefficient than the 2062 Å line. Radiation from the iodine lamp was chopped to provide the signal detected by the PMT. Figure 45 shows the change in signal between HI flowing alone and then with sodium turned on. As sodium reacts with HI, a marked decrease in transmitted radiation at 1830 Å is observed. This indicates the presence of I ($^2P_{3/2}$) atoms within the reacting medium.

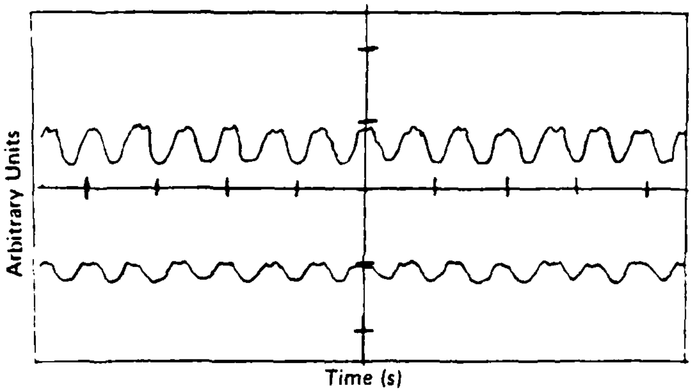

Figure 45. Ground State Iodine Absorption. Upper Trace - HI + He Alone
Lower Trace - Na + He Turned On

Gain tests were then conducted using the double resonance technique. Early program tests appeared to indicate the presence of positive gain in the flow tube. However, extensive further work showed that the interpretation of these early tests was incorrect and that, in fact, loss occurred at all points observed in the tube at all flow conditions used. The error occurred because of difficulties in identifying the baseline for the signal from the photomultiplier tube (PMT) monitoring the resonance lamp.

In order to locate this baseline unambiguously, a dual-beam oscilloscope was used to display simultaneously the outputs of the PMT viewing the 2062Å line and the 1.315 iodine laser pulse. The scope trace was made to start about 2 μs before onset of the discharge in the laser flashlamp. This allowed time for the PMT baseline to be established on the scope trace, even in the presence of the low frequency fluctuation of the 2062Å source intensity.

Flow rates for both the He + HI and He + Na orifices were calibrated so that the actual gas flows during the tests could be ascertained. For the He + Na flow calculations it was assumed that, by the time a volume element of helium reached its orifice, the vapor pressure of sodium reached its equilibrium value (33 torr at 620 C). This should be the case because of the slow flow velocity in the sodium oven. If equilibrium was not established, then the calculated flows are upper limits to the actual flows. The flow tube pressure was monitored at the exhaust end of the aluminum block; typically, it was about 18 torr. A thermocouple was placed just upstream of the optical cavity; measured temperatures of 240 C were typical.

Figure 46 shows typical results obtained by the double resonance technique. The delay between the onset of the sweep and the iodine laser pulse is about 3 μs. In all cases, the PMT signal indicates a downward shift which is in the direction indicating loss rather than gain. Figure 47 substantiates these results. Here the oscilloscope trace was set at 100 microseconds per division. The long decay time is attributed to the rise-time of the PMT-load resistor combination, previously chosen to provide a compromise between sensitivity and speed. (The sensitivity criterion adopted was to be able to detect a 1 percent change in the PMT output.) A photodiode powered by a square wave generator showed the rise-time of the PMT-load resistor combination was about 90 μs.

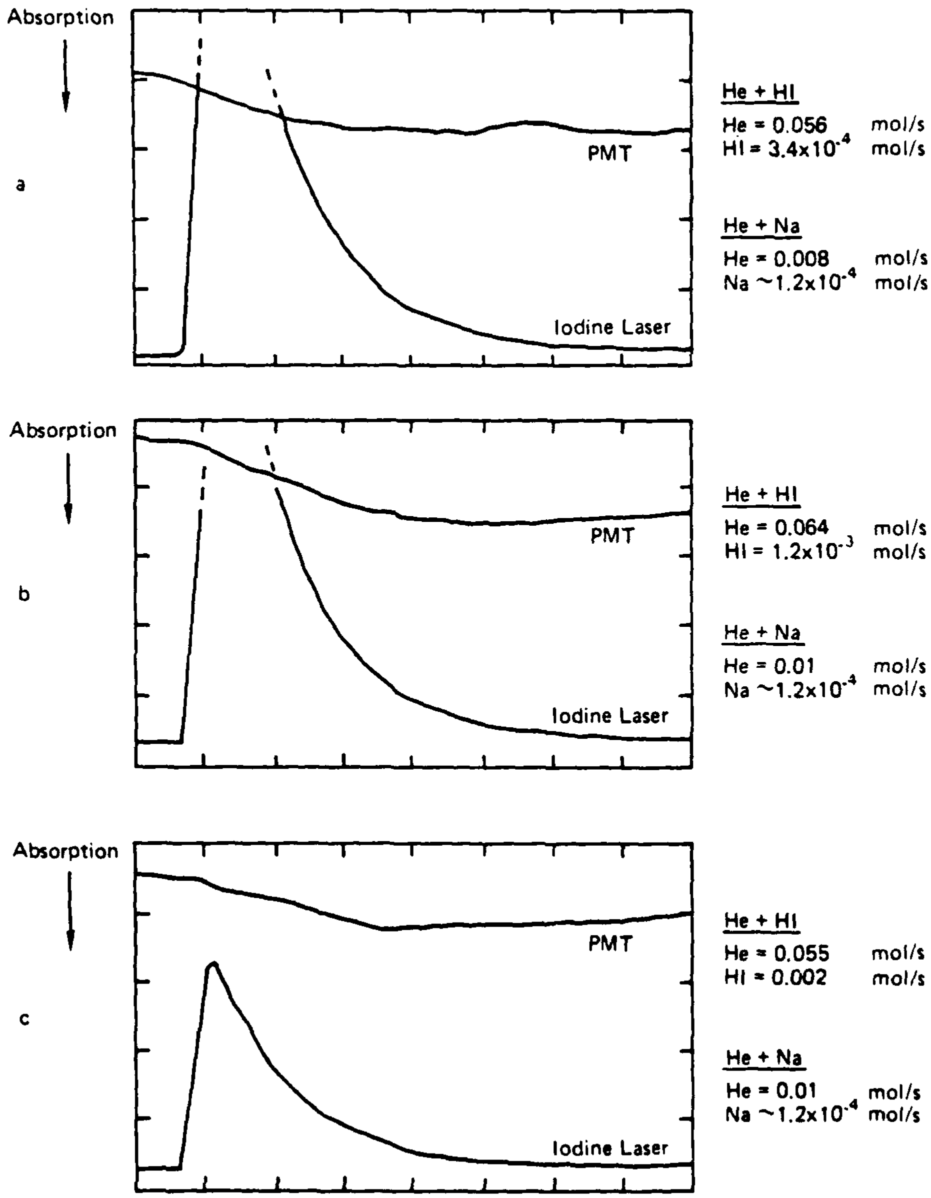

Figure 46. Typical Double Resonance Oscilloscope Traces
5 μs per Div. PMT - 0.5 V/Div.

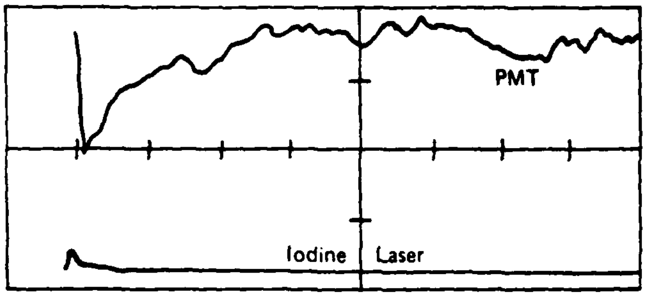

Figure 47. Longer Sweeprate Oscilloscope Trace Depicting Time History of 2062Å Absorption

Sweeprate - 100 μs/div.

MODELING CALCULATIONS

Gain calculations were performed utilizing Bell's BLAZE II computer program. The model consisted of a laminar mixing of two subsonic streams (Mach 0.27). Stream 1 and stream 2 consisted of He + HI and He + Na, respectively. The cases were run at constant pressure.

Figure 48 depicts four cases,one of which (Curve 3) corresponds to the experimental results shown in Figure 46C. Curves 1 and 2 depict the change in gain characteristic when both the sodium and HI flows are increased an order of magnitude. One sees that an increase in flow rates will eventually lead to a condition where no gain can ever be achieved. It appears that decreasing the flow rates (curve 3) quickens the onset of gain. For a given flow rate, however, decreasing pressure prolongs onset of gain.

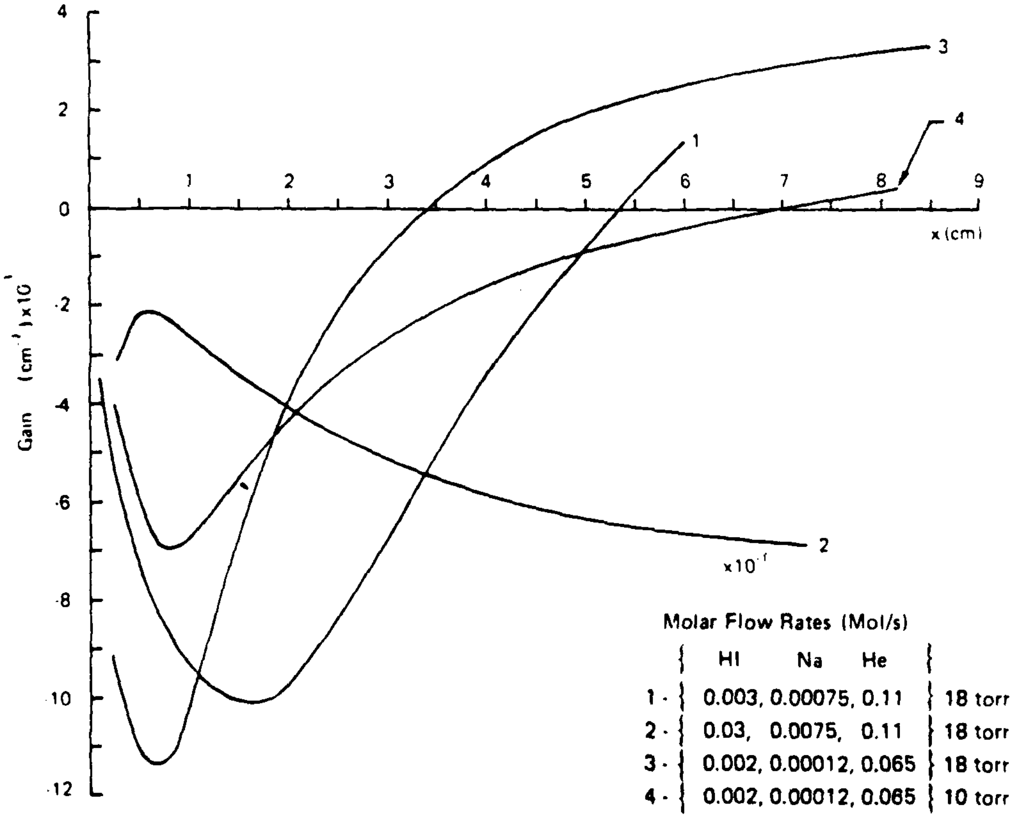

Figure 48. Modeling Results

At this point it is not apparent how to compare the model result shown in curve 3 with the experimental curve shown in Figure 46C. The optical zone between 5 to 6 cm from the nozzle shows loss whereas the model indicates gain ($\sim 2.5 \times 10^{-3}$ cm^{-1}). One surprising feature indicated by the model is that onset of gain takes place at relatively large distances from the nozzle. This being the case would preclude consideration of supersonic devices. This finding also suggests that further measurements be done seeking gain at positions further downstream from the injector. The results of such tests are given in the next section.

GAIN MEASUREMENTS AS FUNCTION OF STREAMWISE DISTANCE

The flow-tube apparatus was modified to allow the position of the He + HI ring injector relative to the gain measurement position to be varied. This was accomplished by mounting the ring injector to a straight tube whose extent within the flow tube could be varied through a compression O-ring seal. This is shown schematically in Figure 49. Gain measurements were done at positions from 2 to 9 cm downstream from the injector. The run conditions are shown in Table XII and the results are plotted versus downstream distance in Figure 50. Although there is apparently substantial scatter in the data, it is evident that loss does occur at all downstream distances and that the loss is increasing (i.e., getting worse) with increasing distance.

These results do not support the modeling calculations, which predict gain under some conditions at rather large distances. This variance could be rationalized if there were some quencher of I* in the flow which is not included in the kinetic model. A prime candidate is NaI, formed in the reaction between Na and HI. When NaI is included in the model as an efficient quencher, loss is calculated at all distances.

On the basis of the above results, it was concluded that the flow-tube as presently configured does not produce a gain medium suitable for sustaining lasing on the iodine atom fine structure transition. Further, the modeling calculations failed to indicate any configuration or flow condition that would produce such a medium. It was therefore decided to abandon the flow-tube and return to the shock-tube to investigate the run conditions that may have given positive gain in the earlier phases of the program (see Table VI).

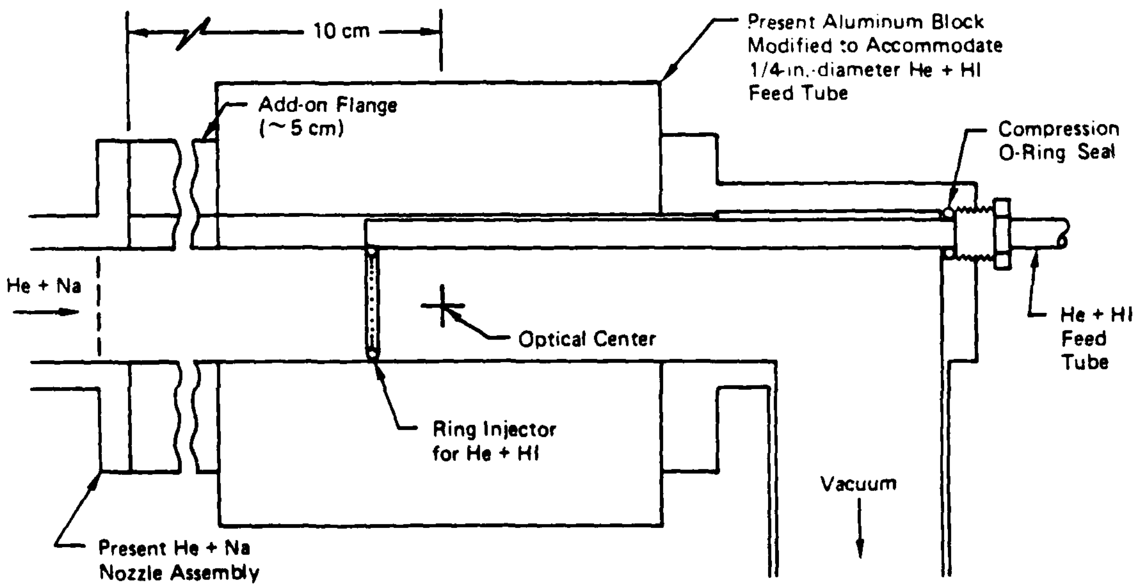

Figure 49. Double Resonance Apparatus Modification

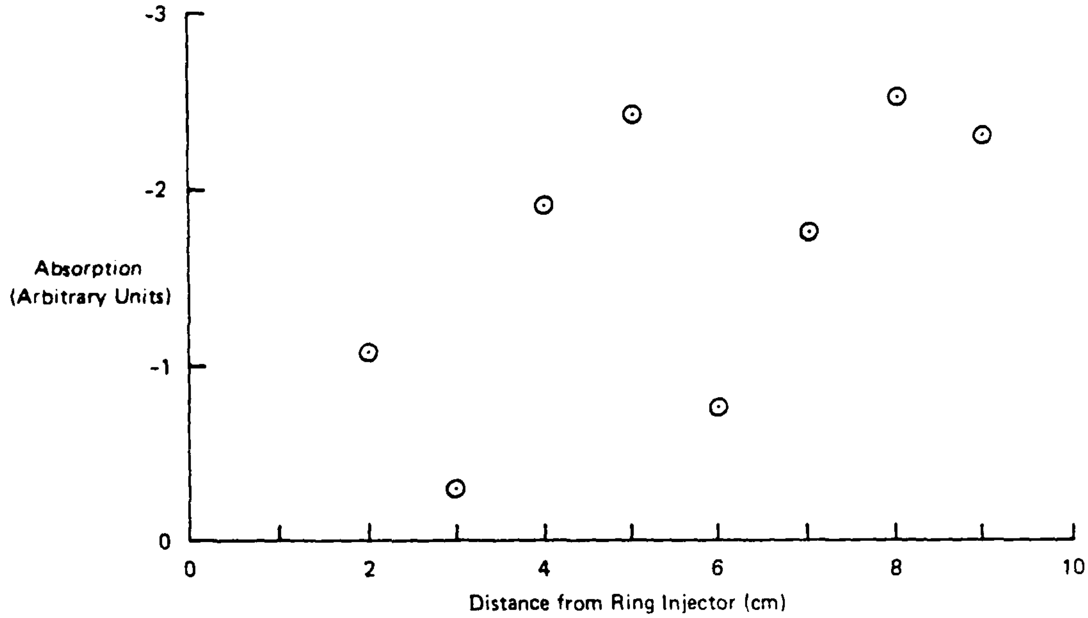

Figure 50. Relative Absorption at 2062Å as a Function of Distance Downstream from Ring Injector

TABLE XII
RUN CONDITIONS FOR THE Na + HI DOUBLE RESONANCE

Distance From Injector (cm)	$\dot{\eta}_{HI}$	$\dot{\eta}_{Na}$	Cavity	
			T K	P(torr)
2	0.002 mol/s	0.12 mmol/s	443	17
3	0.002 mol/s	0.12 mmol/s	433	18
4	0.002 mol/s	0.12 mmol/s	393	18
5	0.002 mol/s	0.12 mmol/s	383	18
6	0.002 mol/s	0.12 mmol/s	378	18
7	0.002 mol/s	0.12 mmol/s	383	18
8	0.002 mol/s	0.12 mmol/s	385	18
9	0.002 mol/s	0.12 mmol/s	383	17

REINVESTIGATION OF SHOCK-TUBE PRODUCED MEDIUM

The double resonance gain apparatus was set up on the shock-tube as shown schematically in Figure 51 and tests were run at conditions shown in Table XIII. The probe laser was placed 8 cm downstream from the nozzle exit plane. The results are shown in Table XIII and plotted versus the ratio of H-atom and HI molar flows in Figure 52. Again only loss is observed and the uncertainties in the results preclude our inferring any definite dependence on the molar flow rate ratio.

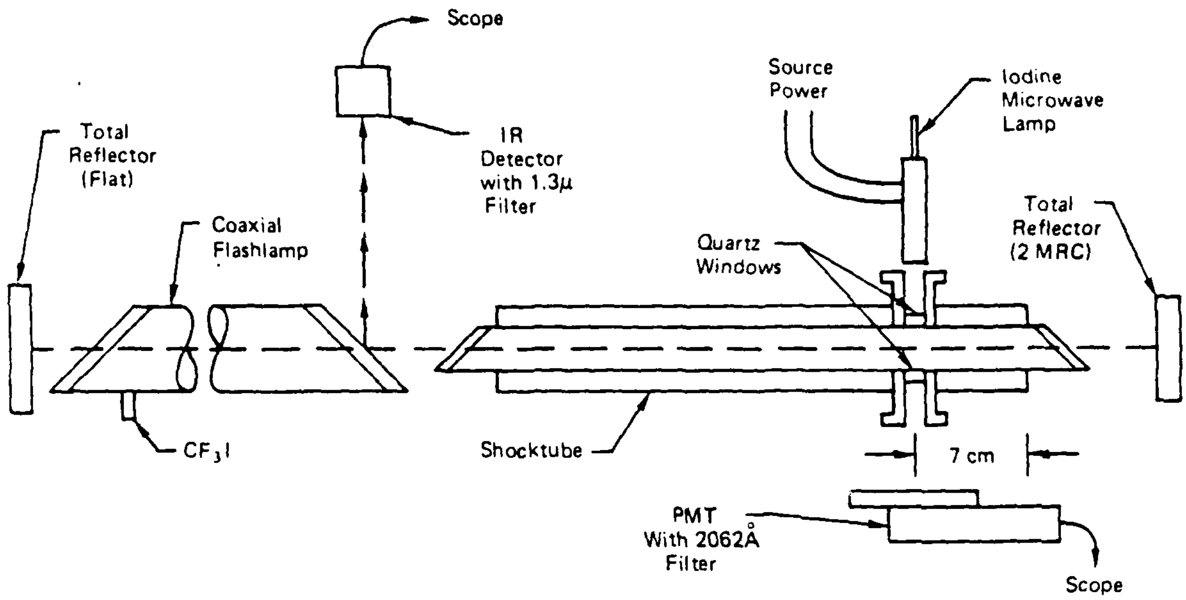

Figure 51. Schematic of Shock Tube Double Resonance Gain Measurement

TABLE XIII. SHOCK TUBE TEST CONDITIONS AND RESULTS

Test	Plenum Conditions		ϕ	$\dot{\eta}_{HI}$	α (cm^{-1})
	T K	P (Atm)			
1	3400	1.6	2.5	0.018	-1.9×10^{-4}
2	3700	2.0	5.1	0.014	-2.9×10^{-4}
3	4100	1.4	4.9	0.018	-1.7×10^{-4}
4	4200	1.5	6.6	0.014	-2.0×10^{-4}
5	4700	1.64	9.6	0.011	-1.4×10^{-4}

$\phi = \dot{\eta}_H/\dot{\eta}_{HI}$

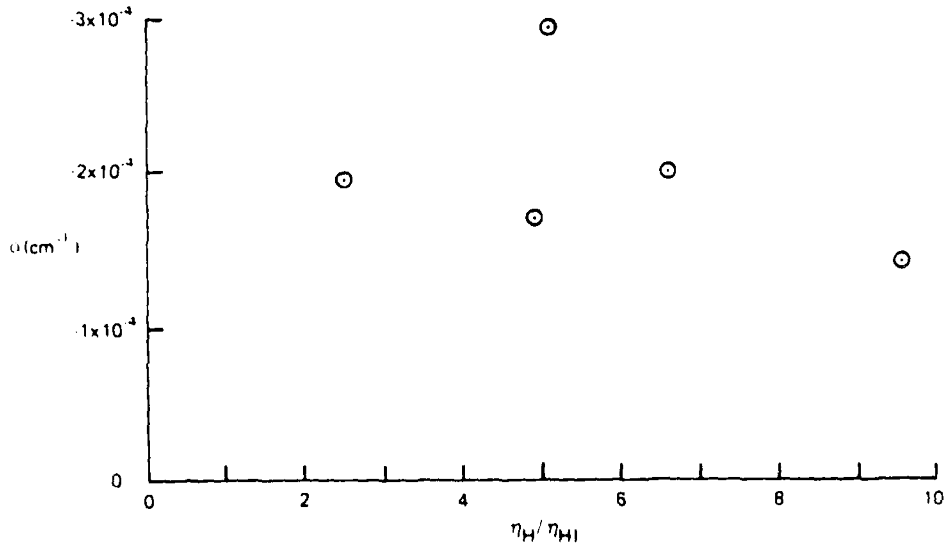

Figure 52. Double Resonance/Shock Tube Results

V. CONCLUSIONS AND RECOMMENDATIONS

1. SHOCK TUBE SUPERSONIC EXPERIMENTS (PHASES I AND II)

The comparative results of the two nozzle systems tested on the 3-in. system show that a steady state of concentration is achieved for the slot nozzle arrangement whereas significant start-up transients are apparent for the nozzle array. This transient phenomenon can be explained on the basis of a wave analysis of the gas interactions occurring within the nozzle. The difference in behavior exhibited by the two nozzle systems is due chiefly to their different expansion ratios.

One other significant difference between the two nozzle systems can be ascribed to the level of hydrogen atom recombination to be expected in each. Thus, the steady state level of radiant intensity given by the nozzle array (after passage of the initial transient pulse) is much lower than that given by the slot nozzle arrangement. An analysis of the problem for the 12-in. system shows that significant H-atom recombination is to be expected on the exposed metallic surfaces during expansion. In the case of the slot nozzle, the walls of the supersonic section are continuously flushed with HI making surface recombination less likely. In spite of this more favorable circumstance, a material balance between the HI injected and the total measured concentration of atomic iodine indicates that at best about 20% of the initial reagent reacts with atomic hydrogen, see Table III(b). This suggests that most of the hydrogen atoms have recombined before they pass the nozzle throat. This is in keeping with a simple analysis of the problem which suggests that in excess of 70% of the losses to recombination occur during the subsonic stages of expansion. The only apparent incongruity to this argument left is that during the initial transient the nozzle array gives results indicative of up to 70% reaction of the HI injected, see Table IV. When viewed in terms of a typical wave diagram, however, this result is easily explainable. Thus, during the initial transient, the pressure and temperature within the cavity will tend to be much higher than is to be expected after establishment of a steady state. Both conditions would act to give anomalously high radiant intensities. Thus, a higher temperature would cause partial dissociation and reaction of the HI present, i.e.,

$$HI + M = H + I + M$$

$$H + HI = H_2(v) + I$$

$$H_2(v) + I = H_2(v-2) + I^*$$

$$I + M = I^* + M$$

The last reaction, one of thermal excitation, would occur to a significant extent after passage of the entropy interface but before passage of the Q-shock. In addition, the anomolously high pressure would produce absolute number densities that were higher than those calculable from the simple equations describing isentropic expansion through the nozzle.

Although the 12-in. nozzle array with an area ratio of 20 also exhibits a nonsteady behavior, the result becomes less pronounced when the area ratio is reduced to 11, see Figures 19 and 34. Nevertheless, some nonsteady behavior persists at the lower area ratio. However, when one row of primary nozzles (two-row array) is blocked, the remaining transient behavior is reduced considerably, see Figures 27 and 28. This is indicative of a wave interaction between the two supersonic streams which is not considered in the construction of our simple wave diagrams. Finally, although a similarity exists between the behaviors of the 3-and 12-in. systems, the overall performance relative to the

HF hot reaction did not scale with size. Thus, at best, a modest decrease in laser power at 2.7 μm is observed on passing from the smaller 3-in. to the larger 12-in. system. This result is in keeping with the nozzle blocking experiments which seem to show that most of the hydrogen atoms delivered to the reaction zone come from the central 4-in. of gas flow through the nozzle, see Figure 26. Again, the result is probably indicative of the different geometries used in the two cases, i.e., single vs double rows of primary nozzles. The scaling difficulty did not, however, extend to the HF cold reaction (see Table VIII).

The results to date indicate that hydrogen atom recombination on the walls of the nozzle are the major difficulty to be overcome in the successful demonstration of the concepts presented herein. Nevertheless, a successful demonstration that the desired chemistry and physics does occur was made. It would appear at this time that only two avenues of approach are open for further studies. Either the nozzle and shock-tube plenum will have to be constructed of or successfully coated with glass (SiO_2) or another nonmetallic material, or, the hydrogen atoms will have to be made in situ by chemical means.

2. SUBSONIC FLOW REACTOR

The 1830Å absorption results show that ground state iodine atoms are produced in the flow reactor but no direct test for the presence of excited iodine could be carried out. The double resonance experiments show that if any excited iodine is formed, it is insufficient or decays too fast to result in positive gain on the ($5P^2_{1/2} \rightarrow 5P^2_{3/2}$) iodine atom transition. The modeling calculations suggest that excited iodine is formed but is rapidly quenched by some species, perhaps NaI. No promising directions for apparatus or flow condition modifications could be identified on the basis of the modeling calculations.

3. REINVESTIGATION OF SHOCK-TUBE MEDIUM (PHASE III)

Since estimates of gain obtained on the basis of admittedly less precise measurements in Phase II suggested that positive gain might have been obtained at some flow conditions, the shock tube medium was reinvestigated to prove or disprove gain at these conditions. The negative results obtained strongly indicate that positive gain was never obtained using the shock-tube. Again, BLAZE II calculations have not indicated fruitful directions for further experimentation.

RECOMMENDATIONS

It seems clear from the collected results of this program that pumping of iodine by H_2^+ does not lead to a useful laser medium and further investigation of the system should be suspended.

REFERENCES

1. D.J. Eckstrom, S.A., Edelstein, and S.W. Benson, J. Chem. Phys., 60, 2930 (1974).

2. R.H. Obenauf, C.J. Hsu, and H.B. Palmer, J. Chem. Phys. 58, 4693 (1973).

3. P. Cadman and J.C. Polanyi, J. Phys. Chem., 72, 3715 (1968).

4. M.L. Zwillengerg, D.W. Naegeli, and I. Glassman, Comb. Sci. Tech., 8, 237 (1974).

5. L.H. Hall, Appl. Phys. Lett., 27 (6), 335 (1975).

6. R.C. Oldenborg, J.L. Gole, and R.N. Zare, J. Chem. Phys., 60, 4032 (1974).

7. M. Polanyi, "Atomic Reactions," Williams and Norgate, London, 1932.

8. H. Beutler and M. Polanyi, Z. Physik. Chem., B1, 3 (1928).

9. D. Husain and R.J. Donovan, Adv. Photochem., Vol. 8, pp 1-75, 1971.

10. D.E. Obrien and J.R. Bowen, J. Appl. Phys., 42(3), 1010 (1971).

11. J.V.V. Kasper and G.C. Pimentel, Appl. Phys. Lett., 5, 231 (1964).

12. K. Hohla and K.L. Kompa, Appl. Phys., Lett., 22(2), 77 (1973).

13. J.V.V. Kasper, J.H. Parker, and G.C. Pimentel, J. Chem. Phys., 43, 1827 (1965).

14. P.J. Kuntz, E.M. Nemeth, J.C. Polanyi, S.D. Rosher, and C.E. Young, J. Chem. Phys., 44, 1168 (1968).

15. T.D. Padrick and R.E. Palmer, J. Chem. Phys., 62, 3350 (1975).

16. S.W. Benson and T. Fueno, J. Chem. Phys., 13, 1597 (1962).

17. D. Britton, J. Davidson, W. Gehman, and G. Schott, J. Chem. Phys., 25, 804 (1965).

18. R.W.F. Gross and J.F. Bott, "Handbook for Chemical Lasers," pp 33-94, Wiley Interscience, New York, 1976.

19. J.A. Blauer, Chemically Pumped Atomic Laser Study, AFWL-TR-75-121, Air Force Weapons Laboratory, Kirtland Air Force Base, New Mexico, March 1975.

20. R.F. Heidner and J.V.V. Kasper, Chem. Phys. Letters, 15, 179 (1972).

21. A.F. Trotman-Dickenson and G.S. Milne, "Tables of Bimolecular Gas Reactions," NSRDS-NB 59, U.S. Dept. of Commerce, 1967.

22. K.F. Herzfeld and T.A. Litovitz, "Absorption and Dispersion of Ultrasonic Waves," pp 281-282, Academic Press, New York, 1959.

23. William L. Wolfe, "Handbook of Military Infrared Technology," pp. 457-518, U.S. Govt Printing Office, 1965.

24. V.S. Zuev, V.A. Katulin, V. Yu Nosach, and O. Yu. Nosach, Sov. Phys., JETP, 35, 870.

25. George Rudinger, "Nonsteady Duct Flow and Wave-Diagram Analysis," pp. 163-168, Dover Publications, Inc., New York, 1969.

26. B.H. Armstrong, J. Quant. Spectr., Radiative Transfer, 7(1), 61 (1967).

27. L.H. Sentman, M. Subbiah, S.W. Zelazny, "BLAZE II: A Chemical Laser Simulation Computer Program," Tech. Rpt. H-CR-77-8, MIRADCOM, Feb. 1977.

28. H. Mirils, "Attenuation in a Shock-Tube Due to Unsteady Boundary-Layer Action," NACA Report 1333, 1957.

29. S. Byron and N. Rott, "On the Interaction of the Reflected Shodk Wave with the Laminar Boundary on the Shock-Tube Walls," Proceedings of the 1961 Heat Transfer and Fluid Mechanics Institute, Stanford, Calif., p. 38.

30. R.B. Bird, W.E. Stewart, and E.N. Lightfoot, "Transport Phenomena," John Wiley and Sons, Inc., New York 1960, p. 529.

31. H. Schay, Z. Phys. Chem., 11B, 291 (1930)

32. M. Polanyi, "Atomic Reactions," William and Norgate Co., London, (1932).

33. A.T. Pritt et al, Appl. Phys. Lett. 31, 745 (1977).

ABBREVIATIONS AND SYMBOLS

ν	Vibrational quantum number
$^2P_{1/2}$	Spectroscopic symbol for upper laser state
$^2P_{3/2}$	Spectroscopic symbol for lower laser state
*	Designates an internally excited atom or molecule - vibrational or electronic
T_o	Initial temperature
P_o	Initial pressure
T	Temperature
P	Pressure
γ	Ratio of heat capacities, C_p/C_v
Å	Angstrom length (10^{-8} cm)
$[I(^2P_{3/2})]$	Concentration of lower laser level
$[I(^2P_{1/2})]$	Concentration of upper laser level
I_o	Initial intensity of resonant radiation
I	Transmitted intensity of resonant radiation
ϵ	Molar absorption coefficient
ℓ	Optical path length
λ	Wavelength
N_u	Number density in upper laser level
V	Voltage
R′	Instrument responsivity
A	Einstein coefficient for spontaneous emission
h	Planck constant = 6.626×10^{-27} erg s
c	Speed of light = 2.9979×10^{10} cm/s

ABBREVIATIONS AND SYMBOLS (CONTINUED)

a	Cross-sectional area of detector active element
Wh	Aperture cross-sectional area at the window
L	Distance from window aperture to the detector
$g(\|\lambda_o-\lambda\|)$	The filter transmissivity at λ when centered at λ_o
ΔL	The optical pathlength through the active medium
N_λ	The black-body radiancy at wavelength λ and temperature T
Γ_X	Molar flow rate of species X (mol/s)
A^*	The effective nozzle throat area
R	The gas constant
M	Molecular weight of gas
α	Small signal gain in units of cm^{-1}
ϕ_c	The line function parameter
ω_c	The line center frequency in units of cm^{-1}
gu	Electronic degeneracy of upper state
g_ℓ	Electronic degeneracy of lower state
ϕ	Molar ratio of HI to atomic H flow
X	Mole fraction of flowing gas
δ_j	Boundary layer thickness in flow Region j
u_j	Gas flow velocity in Region j
U_s	Shock velocity
ν_j	Kinematic viscosity in Region j
τ	Elapsed time
ξ	Distance from origin of disturbance

END

DATE
FILMED

3-82

DTIC